THE DISSOCIATION OF CO*

A. R. Fairbairn

RESEARCH REPORT 305
December 1968

*This research was jointly sponsored by Advanced Research Projects Agency, Department of Defense, ARPA Order #1082 and the Advanced Research Projects Agency of the Department of Defense and Space and Missile Systems Organization, Air Force Systems Command and was monitored by Space and Missile Systems Organization, Air Force Systems Command under Contracts AF 04(694)-695, AF 04(694)-9[illegible] and F04701-68-C-0036.

AVCO EVERETT RESEARCH LABORATORY
A DIVISION OF AVCO CORPORATION

MISSING PAGE
NUMBERS ARE BLANK
AND WERE NOT
FILMED

SAMSO-TR-68-398 RESEARCH REPORT 305

THE DISSOCIATION OF CO*†

by

A. R. Fairbairn

December 1968

AVCO EVERETT RESEARCH LABORATORY
a division of
AVCO CORPORATION
Everett, Massachusetts

*This research was jointly sponsored by Advanced Research Projects Agency, Department of Defense, ARPA Order #1092 and the Advanced Research Projects Agency of the Department of Defense and Space and Missile Systems Organization, Air Force Systems Command and was monitored by Space and Missile Systems Organization, Air Force Systems Command under Contracts AF 04(694)-690, AF 04(694)-983 and F04701-68-C-0036.

†Accepted by Proc. of Royal Soc.

FOREWORD

Distribution of this document is unlimited. This indicates document has been cleared for public release by competent authority.

"This research was jointly sponsored by Advanced Research Projects Agency, Department of Defense, ARPA Order #1092 and the Advanced Research Projects Agency of the Department of Defense and Space and Missile Systems Organization, Air Force Systems Command and was monitored by Space and Missile Systems Organization, Air Force Systems Command under Contracts AF 04(694)-690, AF 04(694)-983 and F04701-68-C-0036." The secondary report number as assigned by AERL is Avco Everett Research Report 305. The Air Force program monitor is Major Walter D. McComb, Jr., SMYSE.

Publication of this report does not constitute Air Force approval of the report's findings or conclusions; it is published only for the exchange and stimulation of ideas.

Major Walter D. McComb, Jr.
SMYSE

ABSTRACT

The dissociation of carbon monoxide diluted with noble gases has been studied in a shock tube. The reaction is complex and appears to be a chain with C_2 as the important intermediate. At temperatures around $8000^{\circ}K$, the reaction rates found to be consistent with the data are $O + C + M \rightarrow CO + M$, $k_r = 2 \times 10^{-34}$ cm^6 sec^{-1}; $C + C + M \rightarrow C_2 + M$, $k_r = 3 \times 10^{-33}$ cm^6 sec^{-1}; $C_2 + O \rightarrow CO + C$, $k = 6 \times 10^{-10}$ cm^3 sec^{-1}; and $O_2 + C \rightarrow CO + O$, $k = 5 \times 10^{-10}$ cm^3 sec^{-1}.

TABLE OF CONTENTS

INTRODUCTION

The high temperature chemistry of carbon is of interest in several fields such as combustion and high speed entry into some planetary atmospheres, but little quantitative work has been reported. Since CO is the simplest starting material which is easily handled, it was chosen in this work to determine its suitability as a controlled source of carbon atoms, and this paper will report a study of its dissociation.

With a binding energy of 11.1 ev, it is necessary to provide temperatures greater than 5000°K to cause appreciable dissociation and the shock tube technique was used as the experimental method. The dissociation reactions of most of the permanent diatomic molecules have now been studied in shock tubes. Under favorable conditions rate constants estimated to be within 20%[1] of the correct value have been obtained. It is rate that reported rates differ by as much as an order of magnitude.[2]

For systems consisting of a highly dilute solution of the reactant in inert gas theoretical calculations are now available and the results tend to be in good (a factor of 2) agreement with experiments.[3] It is, however, necessary to know the reaction mechanism and while this is a straightforward matter for homonuclear molecules, heteronuclear molecules may have much more complicated reaction schemes. Such complications have led in the past to uncertain analyses in systems such as NO and have necessitated in more recent experiments very careful data acquisition and interpretation.[4]

EXPERIMENTAL

A 1.5 inch diameter shock tube was used and measurements were made transversely behind the incident shock (about 11 feet from the diaphragm). A dump tank several feet from the observation station prevented wave reflections. The tube was made of pyrex glass and radiant emission measurements were made in the infrared, visible and ultraviolet.

The infrared measurements were made through a calcium fluoride window. This was contoured to fit flush with the inside of the tube and cemented in with an epoxy resin. A 16 inch focal length gold coated concave mirror was used slightly off axis to collect and focus the light onto a gold doped germanium detector. The CO fundamental at 4.6 μ was isolated with an interference filter (Fig. 1). The image magnification was unity and the entrance aperture to the detector 2 mm square. With f/15 or smaller optical apertures the spatial resolution was about 4 mm. The electronic rise time (10-90%) was about 1 μs.

Time integrated spectra were taken in the visible and ultraviolet, with a small quartz spectrograph. The shutter was opened before the arrival of the shock wave and closed later. The spectra were taken through a quartz window or the calcium fluoride window. It was generally necessary to superpose several shocks on one plate. The spectra showed strong C_2 Swan bands, CN violet and atomic carbon radiation and as a result these wavelengths were also monitored.

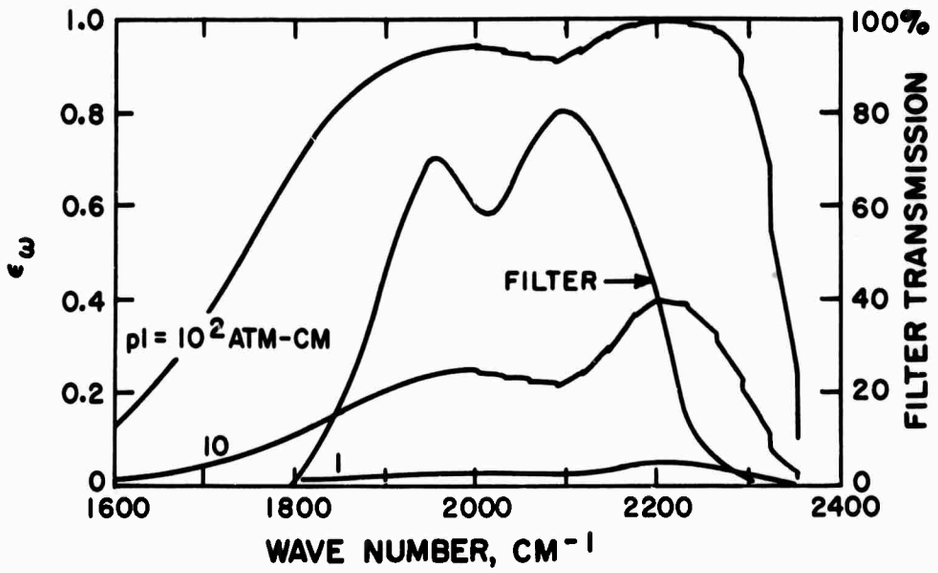

Fig. 1 CO emissivity at T = 5000°K[5] and IR filter transmission characteristics.

A9263

In the visible, the C_2 was followed by a monochromator plus photo multiplier set to receive 5200-5088Å. The CN was followed through an interference filter at 4216Å. In both cases the light was viewed directly through the glass walls of the shock tube.

The atomic carbon line at 2478Å was monitored with an RCA 6903 tube mounted in the focal plane of the small quartz spectrograph. The entrance slit was pushed as close as possible to the window and the optical axis was perpendicular to the tube. The entrance optics were masked down to f/30 giving a spatial resolution of about 2 mm.

Velocity measurements, estimated good to 1/2% were made from the response of thin film heat gauges. These were painted onto plugs cut from the wall of a spare piece of tube. The plugs were placed flush with the inside wall and sealed with epoxy cement. The differentiated signals were displayed on a raster trace on an osiclloscope.

Most of the experiments were made by bursting the diaphragm with cold hydrogen at pressures up to 1400 psi. Some experiments were made with a hydrogen-oxygen driver diluted with helium and ignited by an exploding wire strung down the length of the driver.

Gas mixtures were made from Matheson high purity argon or neon and CP grade carbon monoxide by partial pressure, in a mixing tank, several hours elaspsing before any mixture was used. An early tank of CO had an impurity, which was never identified, with a strong infrared spectrum and which gave anomalous spikes of C_2 at the shock front. The CO used in the experiments reported here did not show this behavior. The only infrared spectra were the CO fundamental and overtone. The main impurity was

nitrogen (460 ppm): Carbon dioxide (350 ppm) and oxygen (150 ppm) were the only other significant impurities.

Initial pressures were generally a few torr and shock speeds up to 5mm/μsec were used giving temperatures from about 5000-10,000°K.

RESULTS

The spectrograms obtained with the small quartz instrument showed the visible region to be dominated by C_2 Swan and CN violet bands. In the ultraviolet the C_2 Mulliken bands, the atomic carbon line at 2478Å and two band systems of CO were identified, the fourth positive bands in the region 2000-2800Å and the (0, 1) band of the Cameron system. Other systems of CO such as the triplet and 3A and Asundi were sought but never positively identified.

Calibration of Infrared System

The infrared system was sensitive enough to be used with mixtures diluted to 0.5% CO + 99.5% Ar or Ne and initial pressures of 5 torr. At lower CO concentrations the signal to noise ratio was too low for meaningful data to be obtained.

Calculations showed that even at the greatest CO density used the intensity of infrared radiation at temperatures greater than 4000°K was proportional to the temperature, and the number of molecules, i.e., the line emissivity, was $\ll$ unity. The detector and recording system should have a linear response. An overall check was made, and the results are shown in Fig. 2 where the results encompass a temperature range from 4000-6000°K. (In the analysis of runs in which reactions occurred, only relative measurements were made.) The experiments were made well in the linear part of the curve ($p_1 \phi \Delta T. \ 10^{-6} < 5$ where p_1 is initial pressure

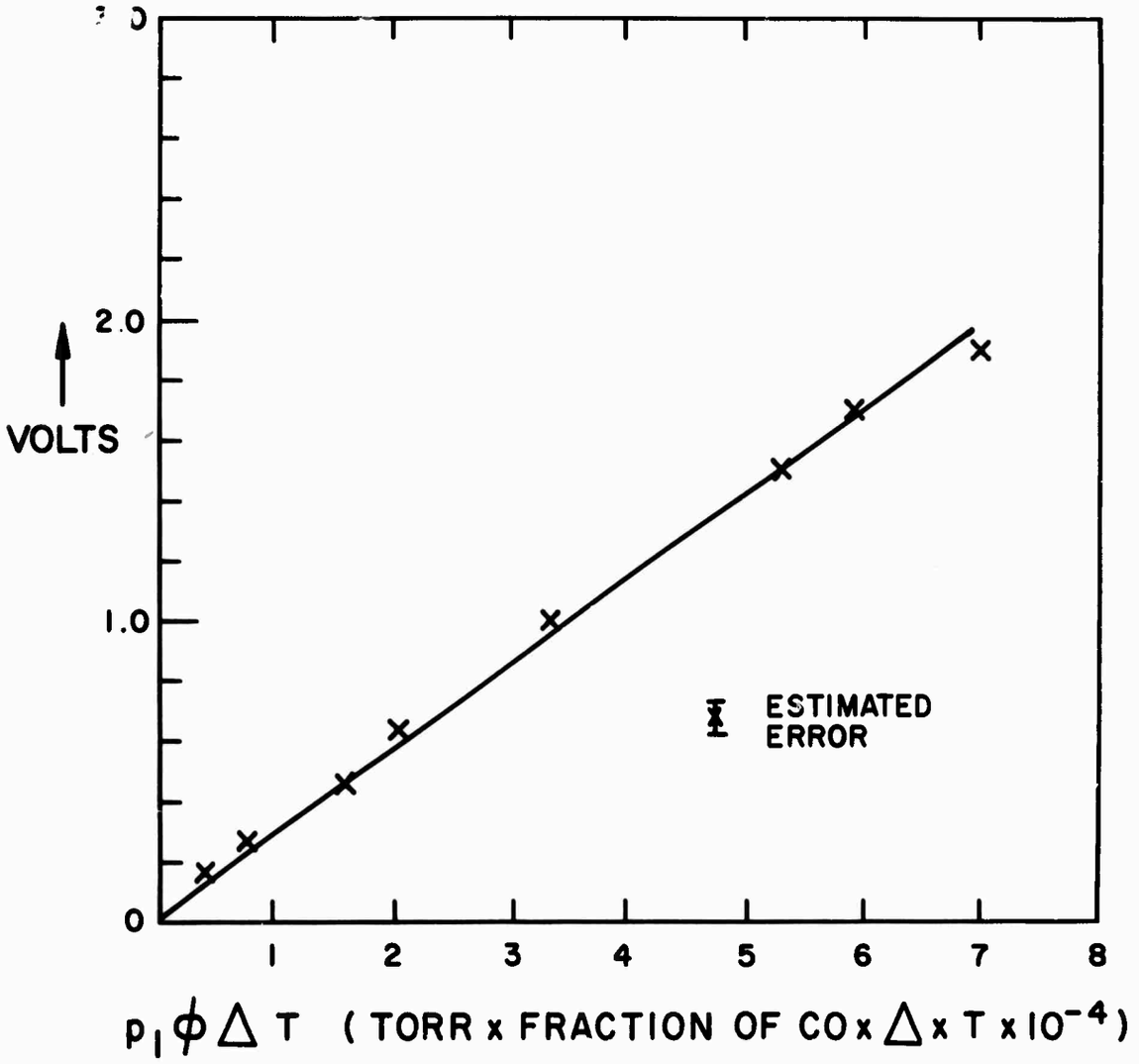

Fig. 2 IR detector system output. The abscissa is in units of torr x fraction of CO x density jump x T x 10^{-4}.

A9266

in torr, ϕ is fraction of CO x 100, Δ is the density jump, T is the temperature.) Figure 2 correlates data up to 10% CO in Ar. It was found that pure CO runs did not scale in this way, being apparently self-absorbed. The addition of argon pressure broadened the lines enough to make them optically thin.

Vibrational Relaxation

The data of Hooker and Millikan[6] show that at temperatures above about 5000°K in the present experiments the vibrational relaxation time will be less than the rise time of the experiment and will be unresolved. For a given run and under conditions of constant pressure behind the shock and large dilution, the infrared signal will be proportional to the fraction of original CO present.

At low temperatures it was found possible to follow the CO vibrational relaxation and the results were in good agreement with the results of Hooker and Millikan. At higher temperatures the rise time became limited by the apparatus and at still higher temperatures (around 6000°K) the CO concentration began to drop off behind the shock front.

Incubation Times

The dissociation of the CO as observed did not occur directly behind the shock front as expected but after a noticeable incubation time. With increasing temperature and pressure the incubation time became shorter. The incubation times are shown in Fig. 3. Most of the data on these incubation times were obtained with argon mixtures and frequently no measurable slope was displayed during the incubation. Some runs made with neon did show an initial decrease in the infrared trace during the

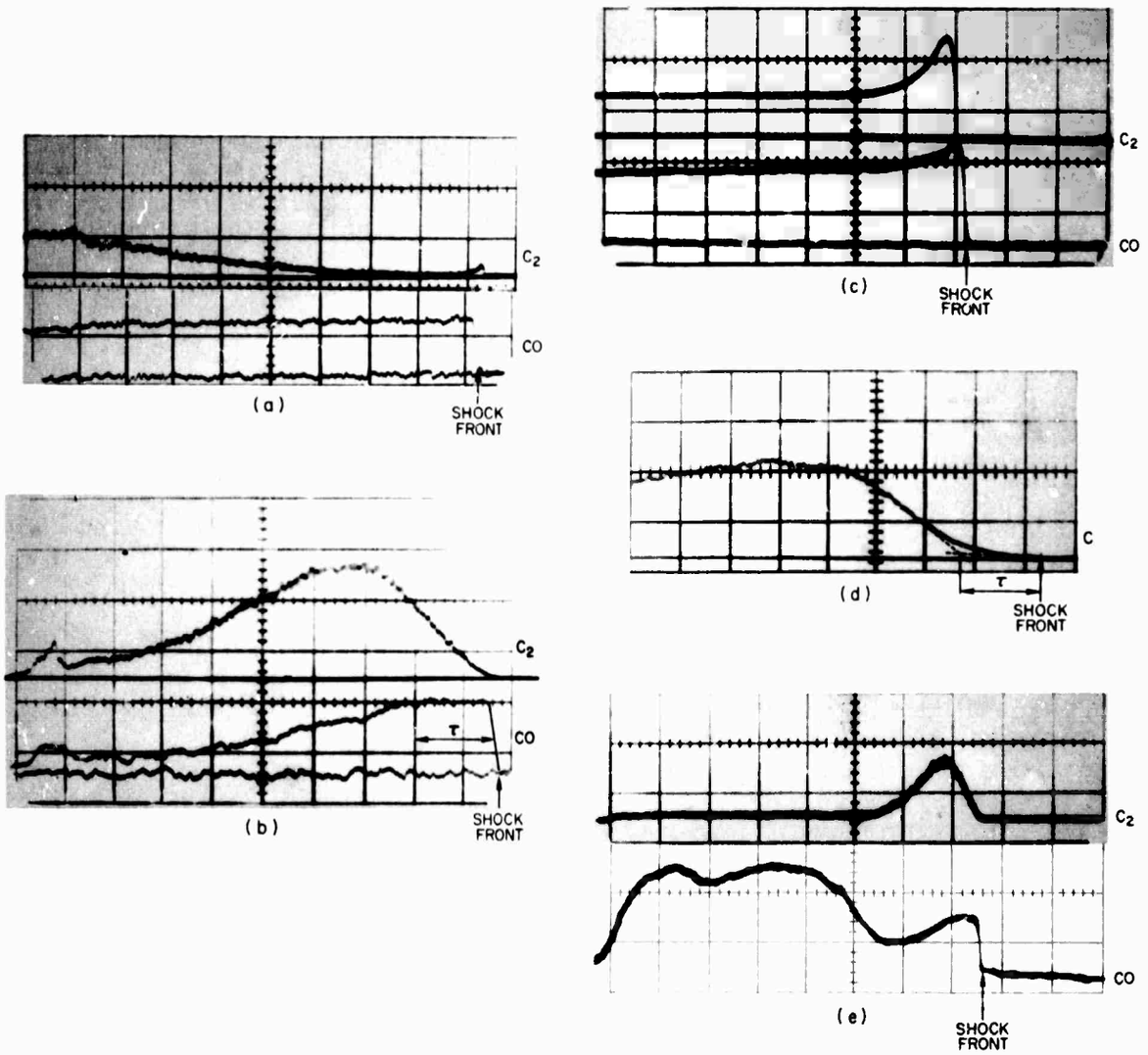

Fig. 3a 1% CO in Ar, p_1 = 10 torr, U_s = 2.47 mm/μs. Lower trace, IR 5 μ ; Upper trace, visible 0.5 μ : time base 20 μ s/div.

b 2% CO in Ar p_1 = 3.1 torr, U_s = 2.97 mm/μs. Lower trace, IR 5μ ; Upper trace visible 0.5μ, time base 10μs/div.

c 10% CO in Ar p_1 = 20 torr, U_s = 3.07 mm/μs. Lower trace, IR 5μ ; Upper trace, visible, 0.5μ ; time base 10 μs/div.

d The same run as (b).
Trace, UV 2478Å , time base 10 μs/div.

e 1% CO in Ar p_1 = 10 torr, U_s = 3.02 mm/μs. Lower trace, visible 0.5μ ; Upper trace IR 5μ, time base 20μs/div.

incubation time. With the incubation times as defined in Fig. 3, Fig. 4 was constructed to correlate the results.

Concurrent observations on the atomic carbon line showed a slow rise followed by a faster one, Fig. 3d. The incubation times data obtained from such traces are given in Fig. 4c. The agreement obtained in the same experiment of incubation times from UV and IR measurements was never perfect but always within a factor of two, which is the experimental scatter. The 2478Å observations were more sensitive at low CO concentrations and enabled incubation data to be obtained at dilutions of 0.02% CO in Ar.

The excitation of the 2478 Å line of carbon in shock tubes is not fully understood and the subject of another report.[7] While the emission level depends on a number of factors it is expected to scale in these experiments with concentration and temperature.

C_2 Bands

The C_2 Swan bands were observed to rise, pass through a maximum which always occurred later than the end of the incubation time, and then fall closely following the CO trace. There was often a small toe at the shock front in the C_2 history indicating a rate of production proportional to time. In quite a number of runs, however, the toe was not very discernable.

The CN violet radiation history was quite similar to that of the C_2 Swan bands. It was only studied as an adjunct to some experiments where nitrogen was deliberately added as an impurity.

Reaction Mechanism

The presence of C_2 shows that the reaction is complex and the shuffle reactions may be important. Unfortunately oxygen does not have a suitable spectral region for study which will not be dominated by other radiation under the conditions of these experiments, and so it was not studied.

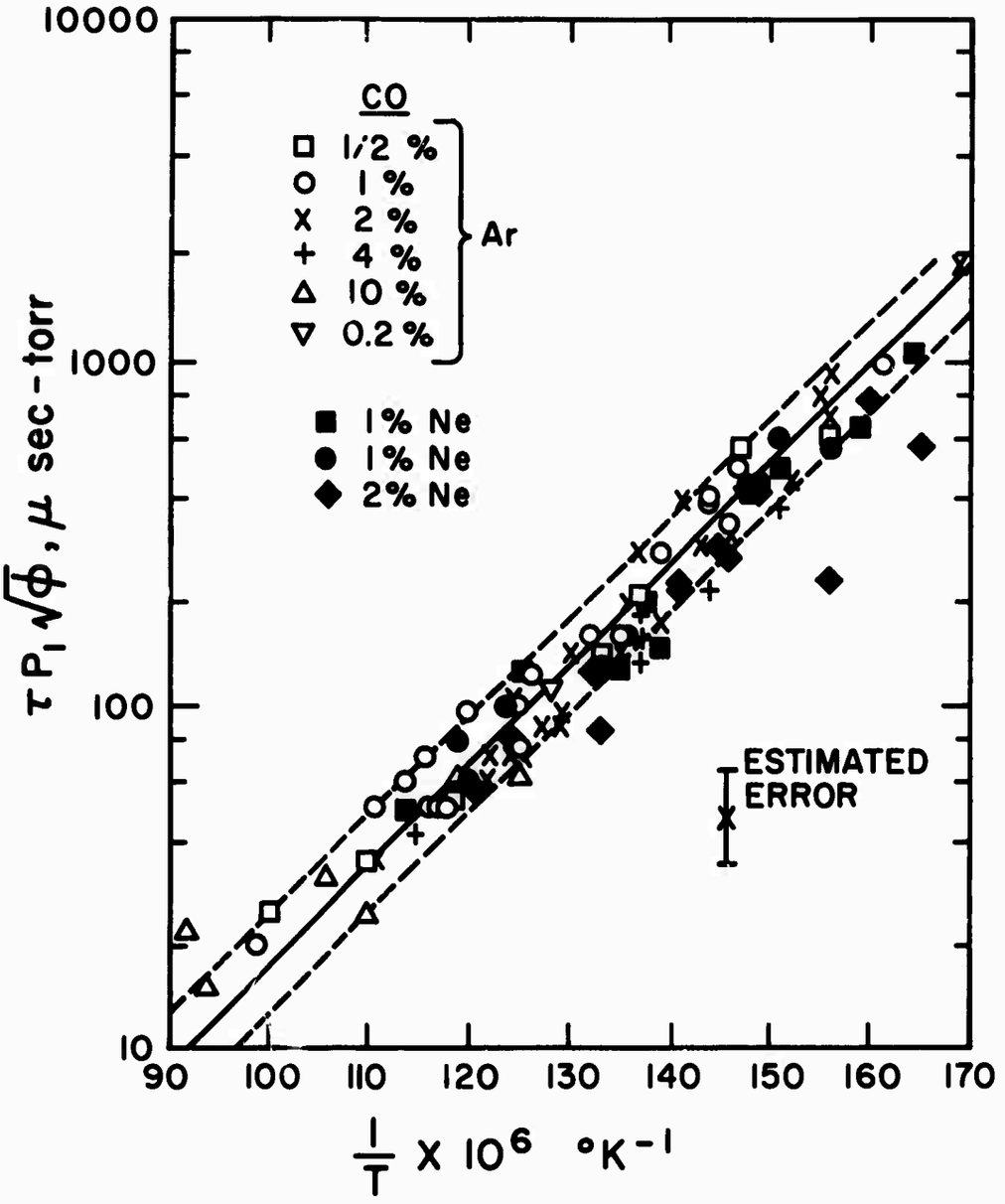

Fig. 4a Incubation times from infrared experiments plotted as function of $\tau p_1 (\phi)^{1/2}$. p_1 is initial pressure (torr), τ is μsec, laboratory time ϕ is 100 times initial fraction of CO.

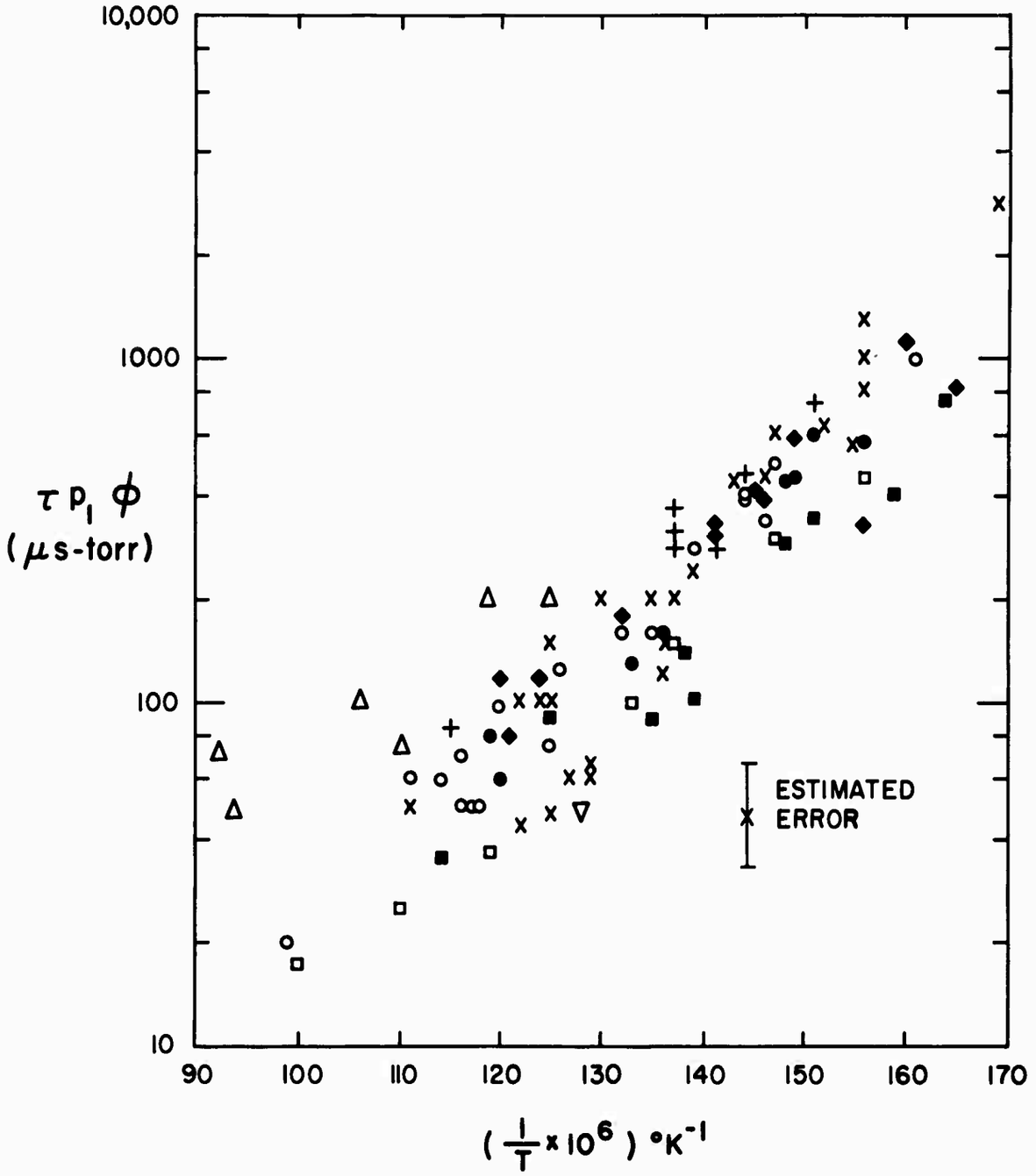

Fig. 4b The same data as in (a) plotted as function of $\tau p_1 \phi$ (a very similar scatter is obtained if τp_1 is used as ordinate).

A9090

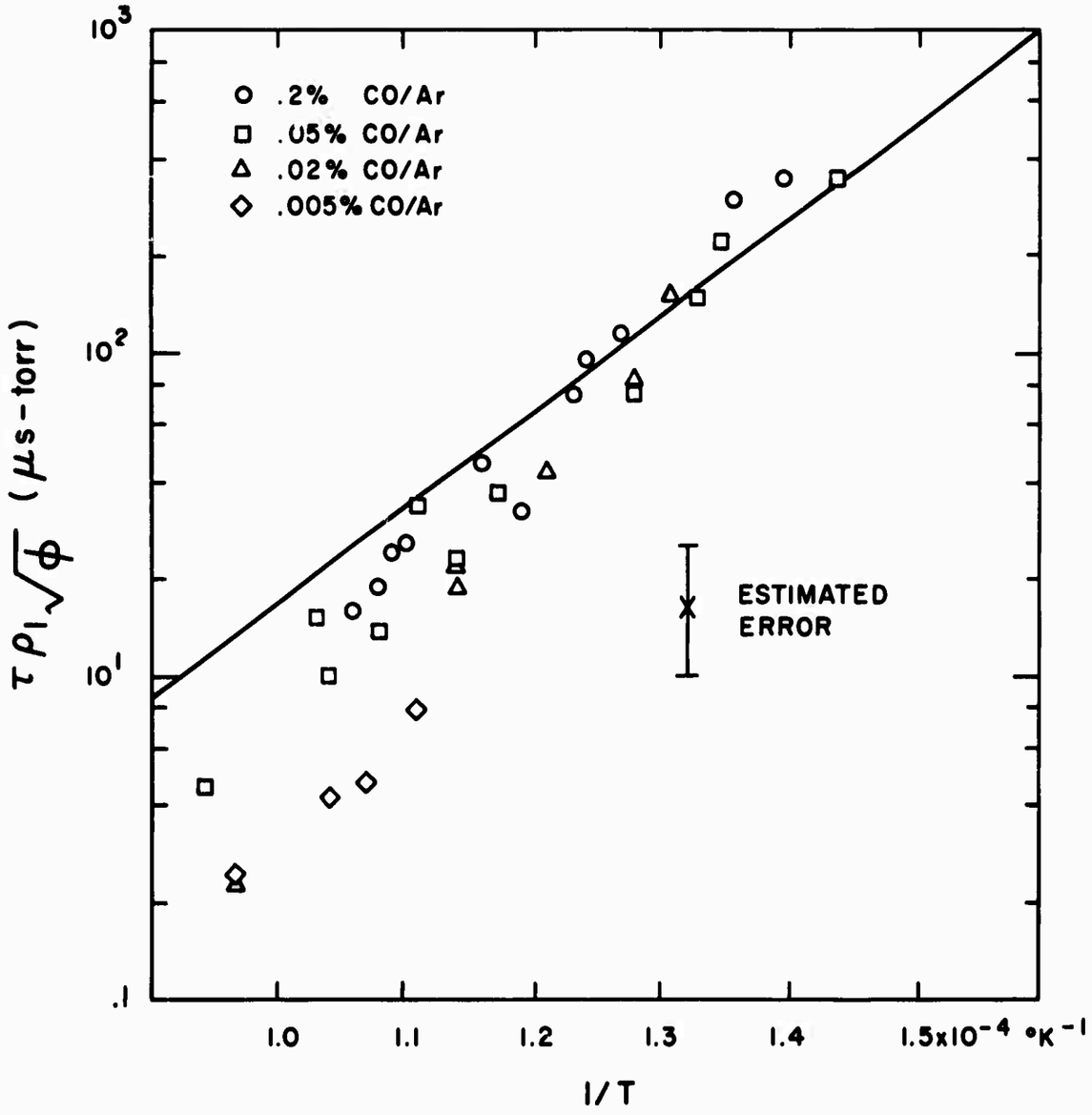

Fig. 4c Incubation times from ultraviolet experiments at 2478Å. The solid line is taken from Fig. 4a.

A9264

By analogy with the chemistry of air[8] the following reactions require consideration:

$$CO + M \rightleftarrows C + O + M \quad (1)$$

$$C + CO \rightleftarrows C_2 + O \quad (2)$$

$$O + CO \rightleftarrows O_2 + C \quad (3)$$

$$C_2 + M \rightleftarrows C + C + M \quad (4)$$

$$O_2 + M \rightleftarrows O + O + M \quad (5)$$

Of these, only the rate of (5) is known. The list is not exhaustive and other reactions are possible. At the high temperatures of these experiments, dissociation reactions predominate and it is felt unlikely that triatomic species will be important routes in dissociation. For instance, the reaction $CO + O_2 \rightleftarrows CO_2 + O$ has been measured[9] but in order to become atomized any CO_2 will have to dissociate again. This matter of triatomic molecule formation will be more fully discussed later on.

The correlations of incubation time shown in Fig. 4 are two of those tried. A plot of $\log \tau p_1$ vs $1/T$ and $\tau p\phi$ vs $1/T$ show similar scatter and it was found that $\log \tau p\phi^{1/2}$ gives the best correlation. The temperatures used are those assuming frozen chemistry, but full vibrational and rotational relaxation. In the dilute mixtures used the density jump at the shock front is always close to 4 and the parameter $p_1\phi$ is a measure of the CO concentration.

The incubation results may be explained on chemical grounds, but it is necessary to first rule out shock attenuation as the cause. Attenuation will have two main effects on the observations. The increasing temperature

behind the front will cause more rapid reaction, particularly in view of the very high activation energy of dissociation of CO. The boundary layer build-up will also, even in the absence of a temperature increase, by shortening the time scale in laboratory co-ordinates cause an apparent increase in reaction rate. But the small fraction of CO in the mixture will not alter the aerodynamics much and the scaling found depending on $\phi^{1/2}$ is not to be expected unless it is due to the chemistry.

Reactions of the type O + CO → O + C + O and C + CO → C + C + O will have an auto catalytic effect but with concentrations of 1% or less of CO integration of these equations together with (1) showed that O or C will need to be about a factor of 1000 faster than argon in the dissociation of CO to give the observed incubation behavior even approximately. This factor is unlikely; comparison with oxygen and nitrogen dissociation shows the effect to be about a factor of 25 or 35.

It thus appears that some diatomic intermediate is formed and this causes the turn over from an initially slow rate to a much faster one. There are three a priori possibilities, O_2, C_2 and CO^* where the asterisk refers to any or all of the triplet states of CO which dissociate to normal products.[10] In order to affect the dissociation rate to give an incubation effect as observed, it is necessary that the intermediate should have a higher cross section for dissociation than the original CO. The Keck-Carrier[4,11] theory of dissociation may be used to estimate that the recombination rate, k_r, for (1) with CO in the ground state is $\sim 10^{-34}$ cm^6 sec^{-1} while for C_2 in the $X^3\Pi$ state it is $\approx 7 \times 10^{-34}$ and for CO^* it is $\approx 10^{-33}$.

The O_2 rate is experimentally determined to be close to 10^{-34}[1*]. Because of the low equilibrium concentration of O_2 in dissociating CO mixtures unless raction (3) is made very fast (>>gas kinetic cross sections) O_2 cannot be the intermediate.

Triplet States of CO

The observation of the Cameron band (0, 1) at 2155Å indicates that triplet states of CO are present, the transition involved being $a^3\Pi \rightarrow X^1\Sigma$. Davies[12] has reported the observation of the triplet bands at 6434Å, due to $d^3\Delta \rightarrow a^3\Pi$, and 3A bands in the ultraviolet. Although they were carefully sought, these triplet and 3A bands were not positively identified in these experiments by photographic means. A series of experiments was run using photoelectric detection. The CO triplet radiation will occur between 4000Å and 9000Å, but the spectrum is dominated between 4000 and 6000Å by C_2 Swan, and CN red will occur between 8000 and 9000Å. Observations were made from 6000 - 12,000Å using Corning filters and a S1 surface photomultiplier. Several combinations were used. Some were broad band and some narrow (500Å). Because of C_2 and CN and continuum radiation, it was not possible to positively identify any radiation as due to the CO triplet states in this region.

The mode of excitation to the $a^3\Pi$ state is a matter of importance but little knowledge. Estimates have been made[13] that the Cameron bands are around a factor of 10^3 weaker than the fourth positive, $A^1\Pi \rightarrow X^1\Sigma$. Recent work[14] has shown the lifetime of the $A^1\Pi$ state to be around 10^{-8} sec and so the radiative lifetime of the $a^3\Pi$ is probably about 10^{-5} sec.

---

*All rates in this paper will be given in particles per cubic centimeter per second units.

Using Hansche's observations on the quenching of the Cameron bands in a discharge it may be concluded that the cross section for the process $CO(^1\Sigma) + CO(^3\Pi) \rightarrow CO(^1\Sigma) + CO(^1\Sigma)$ is close to gas kinetic.[15]

It is unlikely that argon will have a substantial cross section for the deactivation of $CO(a^3\Pi)$, it is probably less than 10^{-2} of gas kinetic and thus unimportant in 1% CO mixtures, compared with CO itself. Atoms, either C or O are not expected to have cross sections significantly greater than gas kinetic, thus in a 1% mixture where less than 10% of the CO has dissociated atoms will still be less important that $CO(^1\Sigma)$ in the deactivation. Radiative deactivation will always set an upper time limit on the achievement of a steady state of $CO(a^3\Pi)$ if the major process involves CO molecules and not atoms. This time is of the order 10^{-5} sec or about 3 μsec in laboratory coordinates. The incubation times were generally much longer than this, indicating that there is no connection between the incubation time and CO^* if Refs. (13) and (15) are correct in their findings.

The incubation time appears most likely to be associated with the formation and dissociation of C_2. It was remarked earlier that the C_2 concentration reached a peak after the end of the incubation time. The absolute concentration of C_2 is always much less than that of CO and so at all times the C and O atom concentration are nearly equal.

The end of the incubation time is noted experimentally to occur when $[C_2]_\tau \approx K_2 [CO]/10$ where K_2 is the equilibrium constant of reaction (2) and the time required to achieve this is $\tau \approx [C_2]_\tau / d[C_2]/dt$. From reactions (2) and (4) $d[C_2]/dt = k_2[CO][C] - k_2^-[C_2][O] - k_4 M[C_2]$, where k and k^-

refer to the forward and backward rate constants, and at early times the second term is not important. The first and third terms are nearly equal and the difference is probably of order $k_2 [CO] [C]/10$. The average of [C] at t is $k_1[CO] [M]t/2$. Thus

$$[C_2]_\tau = \int_0^\tau \frac{k_2 k_1 [CO]^2 [M] t \, dt}{10 \times 2} \approx \frac{k_2 k_1 [CO]^2 [M] \tau^2}{40}$$

hence

$$\tau^2 \approx \frac{4K_2}{k_2 k_1 [M][CO]}$$

since [CO] is taken as constant during the incubation time.

An expression of similar form but different value is obtained by noting that the end of the incubation time will be apparent when

$$d[C_2]/dt \approx 2k_1 [CO][M]$$

from which

$$[C_2]_\tau [M] k_4 \approx 2k_1 [CO][M],$$

as before

$$[C_2]_\tau \approx k_1 k_2 [CO]^2 [M] \tau^2/40,$$

hence

$$\tau^2 \approx \frac{80}{k_2 k_4 [M][CO]}$$

These two expressions for the incubation time are, of course, related by the ratio of k_1 to k_4. [M] is mainly argon and is closely proportional to $p_1 \Delta$, while [CO] is proportional to $p_1 \phi \Delta$. Δ, the density jump across the shock, does not very greatly and so $\tau^2 p_1^2 \phi \approx K_2/k_2 k_1$. It is also

necessary, as mentioned before, for the production of carbon atoms via reactions (2) and (4) to exceed the production from reaction (1) in order to observe the change of slope in the CO trace. Thus, if reaction (2) is fast enough to keep in local equilibrium, the condition for a clearly observed change in slope is $K_2 [CO] [M] k_4 > [CO] [M] k_1$.

In Fig. 4a is plotted $1/2 \log \tau^2 p_1^2 \phi$ vs $1/T$. The slope of this line should be given by $(K_2/k_1 k_2)^{1/2}$. K_2 has an activation energy of 113 K cal/mole while k_2 will probably have a similar activation energy, hence the temperature variation of the incubation time will be close to that of $(1/k_1)^{1/2}$ or 128 K cal/mole. The value obtained from the data is 135 $\pm$ 15 K cal/mole which is considered a satisfactory agreement.

POSSIBLE ALTERNATE INCUBATION MECHANISM

In a previous communication,[16] the author argued that the incubation phenomenon was more probably to be associated with CO^* before becoming aware of the implications of reference.[15] On the basis of the data presented in this paper it is not in fact possible to separate out the possible effect of CO^* if it should turn out to have a much larger lifetime than that assumed (10^{-5}s) or if $CO(^1\Sigma)$ has a very much lower cross section than $O(^3P)$ or $C(^3P)$ for the excitation to CO^*.

Extraneous Effects on the Observations

At the high temperatures used in these experiments there are several effects which can interfere both with the reaction mechanism and with the observations. Fig. 3e demonstrates the effect of ionization of carbon on the infrared signal. The CO emission will tend to zero as the CO dissociates, but the continuum radiation (free bound plus free free) due

to ion-electron and neutral-electron interaction will rise as the gas ionizes at these high temperatures. Because of this effect, it is not possible to follow the CO concentration to the completion of the reaction, and even the initial portions of the trace are distorted.

Another effect which might interfere with a straightforward analysis of the data could be the presence of argon metastable species. These have been shown by Petschek and Byron[17] to be important in the initial ionization of argon by atoms. They occur at an excitation energy of 11.5 ev, which is fairly closely resonant with the dissociation energy of CO, 11.1 ev. To check this possibility some runs were made with neon as the working gas. The lowest metastable levels of neon lie at 16.6 ev, and accidental interference with the dissociation will not occur. The records show that there is little difference between argon and neon as the collision partner. Because the neon has to be driven by combustion, attenuation of the shock wave gave rather larger scatter in the measured incubation time.

Effects of Impurities on the Incubation Time

The effect of impurities on the incubation time was studied in a series of experiments. The additives tested were oxygen, added to replace 5, 20 and 50% of the original CO, nitrogen and carbon tetrachloride to replace 5% of the CO. Carbon per se cannot be added to the CO and the addition of carbon tetrachloride was considered as the easiest means of adding carbon atoms. Unfortunately, it will give four times as many chlorine atoms and while it might be supposed that chlorine atoms will act as an inert diluent, a series of experiments should be run to check this point. Under the conditions of these experiments both O_2 and CCl_4 will be dissociated in much less than the incubation time.

The results are shown in Fig. 5. The three solid lines are taken from Fig. 4a and are for reference only. It will be noted that there is a larger scatter and that nitrogen has no significant effect. There appears to be a general slight shortening of the incubation time with carbon tetrachloride and a lengthening with oxygen additions. While the results are not conclusive, they suggest that carbon atoms do shorten the incubation time.

While the effect of N_2 upon the incubation time was being investigated, its effect on the CN radiation was also studied. As might be expected, addition of N_2 to the mixture strongly enhanced the CN emission but did not change any other radiation.

The Initial Reaction Rate

The majority of the argon diluted experiments did not show an initial slope measurably different from zero. On the other hand runs in neon mixtures tended to give a finite initial slope. This difference in behavior indicates strongly that even at early times ionization is occurring and a rising component of ionization continuum is superposed on the falling CO signal. The substitution of neon for argon will at once tend to give lower ionization levels and since it also has a much smaller cross section for neutral Bremstrahlung[18] the interference with the CO signal will be reduced.

Because of the auto catalytic effect, it is to be expected that the initial slope showed gradual increase and taking into account the noise on the traces and the fact that aerodynamic effects on the temperature can drastically change the reaction rate it is not expected that the initial rate data which was obtained and is presented in Fig. 6 is particularly reliable. In fact, it is probably not better than about a factor of three. The scaling found to give the best representation of the data was $d[CO]/dt = - k_1 [M] [CO]$.

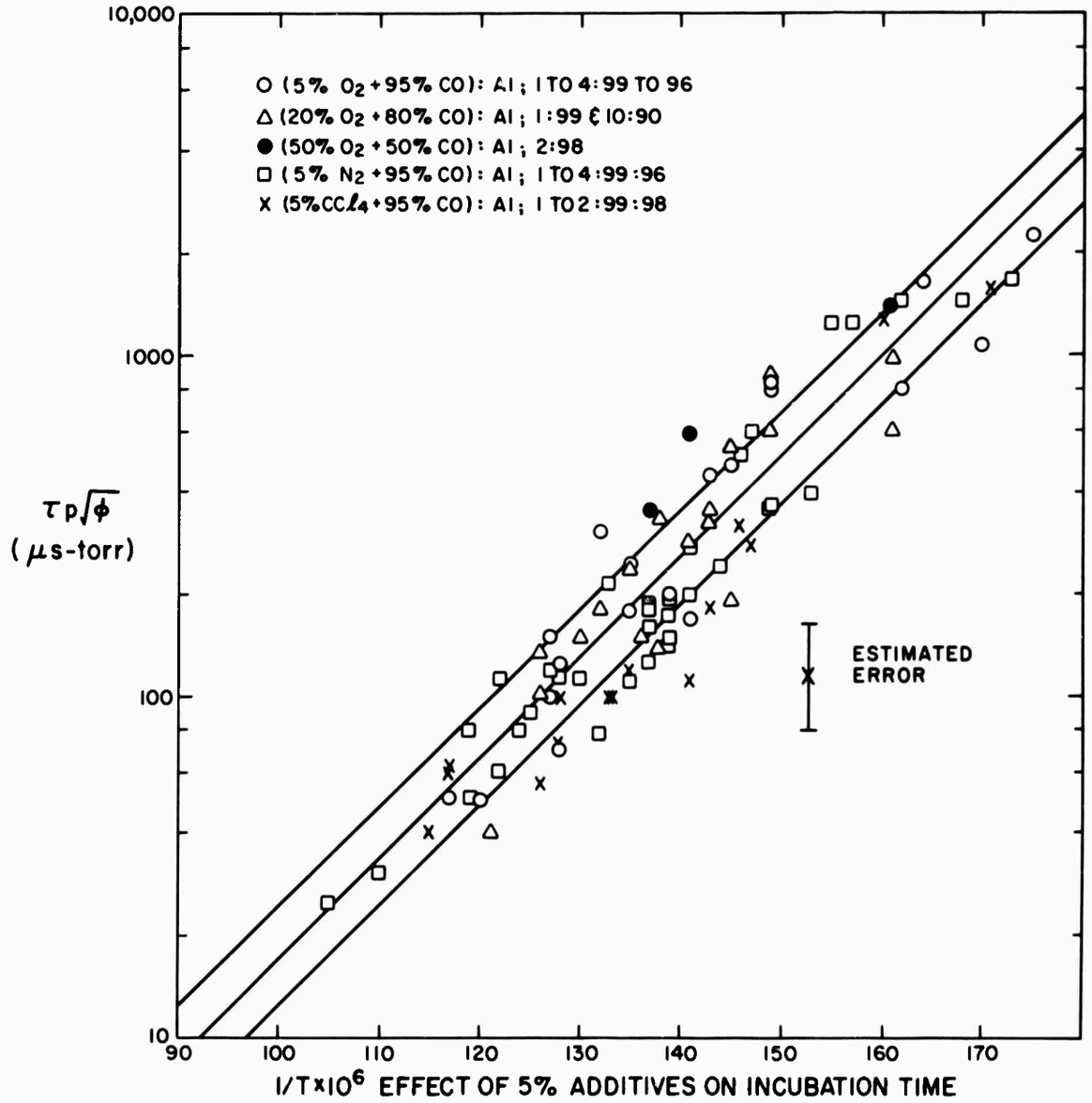

Fig. 5 Effects of impurity addition on incubation time. The lines are taken from Fig. 4a.

A5186

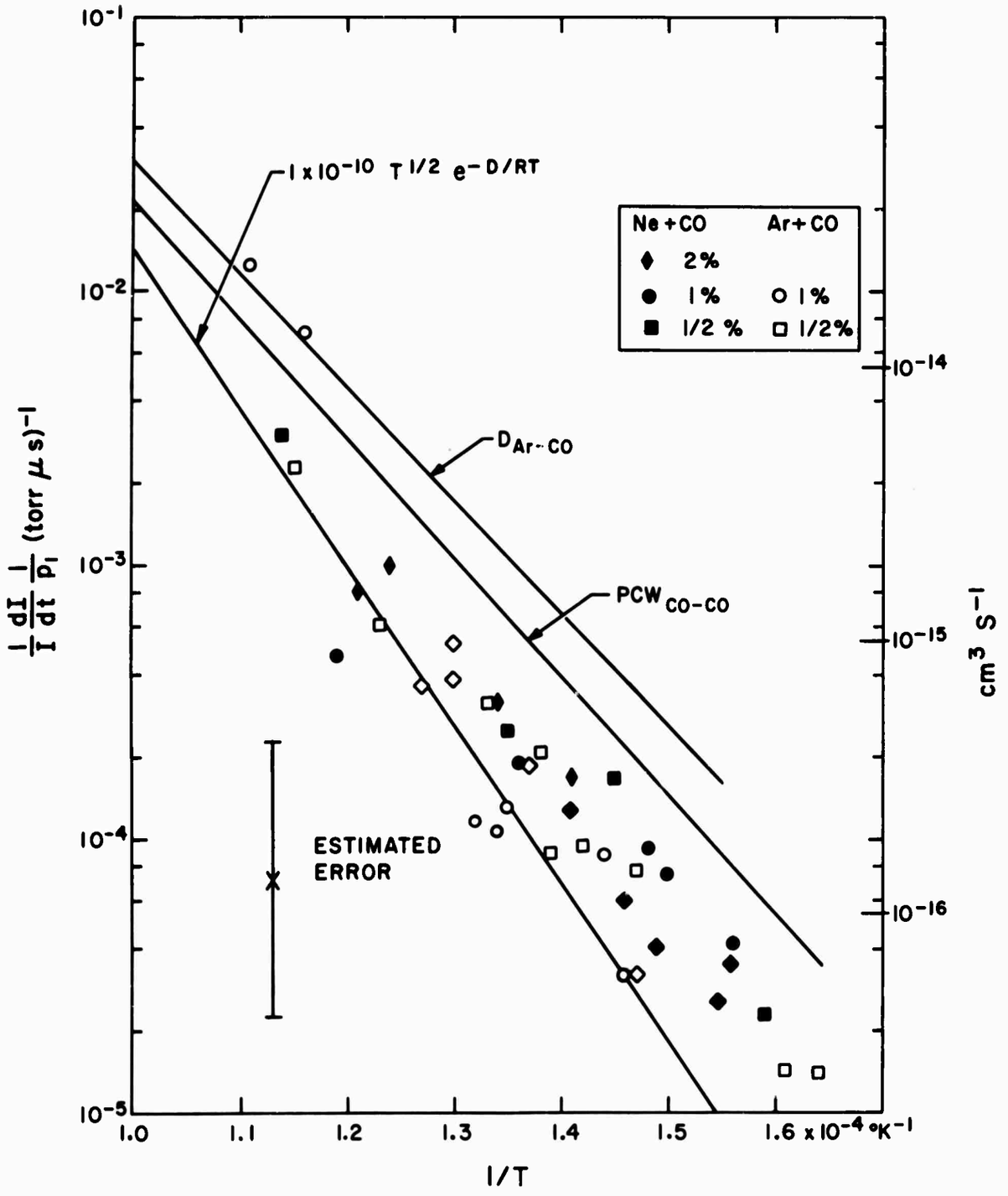

Fig. 6 CO dissociation rates obtained from initial slopes. The line marked D is Davies' rate[12] and PCW is from Presely, Chackerian and Watson.[19]

A9265

The line which was fitted to the data by eye and anticipated the low temperature observations would give rates which were to fast, is represented by $k_1 = 1 \times 10^{-10}(T)^{1/2} \exp(-D/RT)\, cm^3\, s^{-1}$ which is equivalent at 8000°K to a recombination rate constant of $4 \times 10^{-34}\ cm^6\ s^{-1}$. Also plotted in Fig. 6 are lines due to Davies[12] for Ar plus CO mixtures and Presely, Chackerian and Watson[19] for pure CO. From the way in which these authors obtained their rates they should be more properly compared with what will be called the second reaction rate in this paper.

Some of the data presented by Presley, Chackerian and Watson for the infrared emission from dissociating pure CO indicate the presence of an incubation time although the authors do not comment on this. Their shock front temperatures were around 20,000°K. When plotted on Fig. 4a, extrapolating the solid line given, it is found that the CO-CO incubation time is about 50% longer than the CO-Ar (extrapolated) value. This difference lies within the experimental error particularly since shock curvature introduces a significant uncertainty at the low pressures used in the pure CO work. It is improbable that CO-CO collisions are less effective than CO-Ar and the data of Presley, Chackerian and Watson is interpreted here to mean that CO-CO and CO-Ar have comparable cross sections in the dissociation process.

Second Reaction Rate

A temperature change of 100°K can cause a change in reaction rate of 20% in the range of interest. Such a temperature drop can be caused by a fairly small degree of reaction. Acting in the opposite direction attenuation and boundary layer growth will actually cause a temperature rise which may

more than off set the drop due to reaction and given an apparently faster reaction. The data presented in Fig. 7 are affected by these considerations, in particular those taken at the low temperature end. In these the slope was measured some distance behind the shock front and from the known attenuation alone the observed rates at 6500°K are probably a factor of two high. At the high temperature end of the range, ionization begins to cause lower rates to be observed and thus the trend in the data will be to give a lower activation energy than the true value.

It will be noted that the infrared data acquired in the present experiments is in quite good agreement with that of Davies, although the interpretation is entirely different.

In view of the arguments developed concerning the incubation time, it is clear that this second reaction rate probably does not have a large component of CO dissociation, rather it is determined by reactions (2), (3), (4) and (5) and while it can be fitted with a kinetic rate expression referring to [M] and [CO], such procedure has only empirical value.

THE RATIO OF THE INITIAL TO SECOND REACTION RATE

Experimentally it is found that there is about a factor of 6 between the first and second rates at 8000°K. It is also estimated that the C_2 concentration during the final stages of the reaction is about a factor of two below its equilibrium value. The rate of disappearance of CO via reaction (1) is $d[C_2]\ dt = [\dot{CO}]_1 = - k_1 [CO] [M]$ while via reactions (2) and (4) the rate is given by $[\dot{CO}]_2 = - k_2 [CO] [C] + k_2^- [C_2][O]$ and $[\dot{C}_2] = - [CO]_2 - [C_2] [M] k_3$ but since $[\dot{CO}] \gg [\dot{C}_2]$, $[\dot{CO}]_2 \approx - [C_2] [M] k_3$ and substituting $[C_2] \approx K_2 [CO]/2$, (the experimentally observed limit) the result is $[CO]_2 \approx K_2 [CO] [M] k_3/2$. Thus by rearranging $k_3^- \approx 10\ k_1^- K_1/K_2 K_3$ and at 8000°K, $k_3^- \approx 10\ k_1^-$.

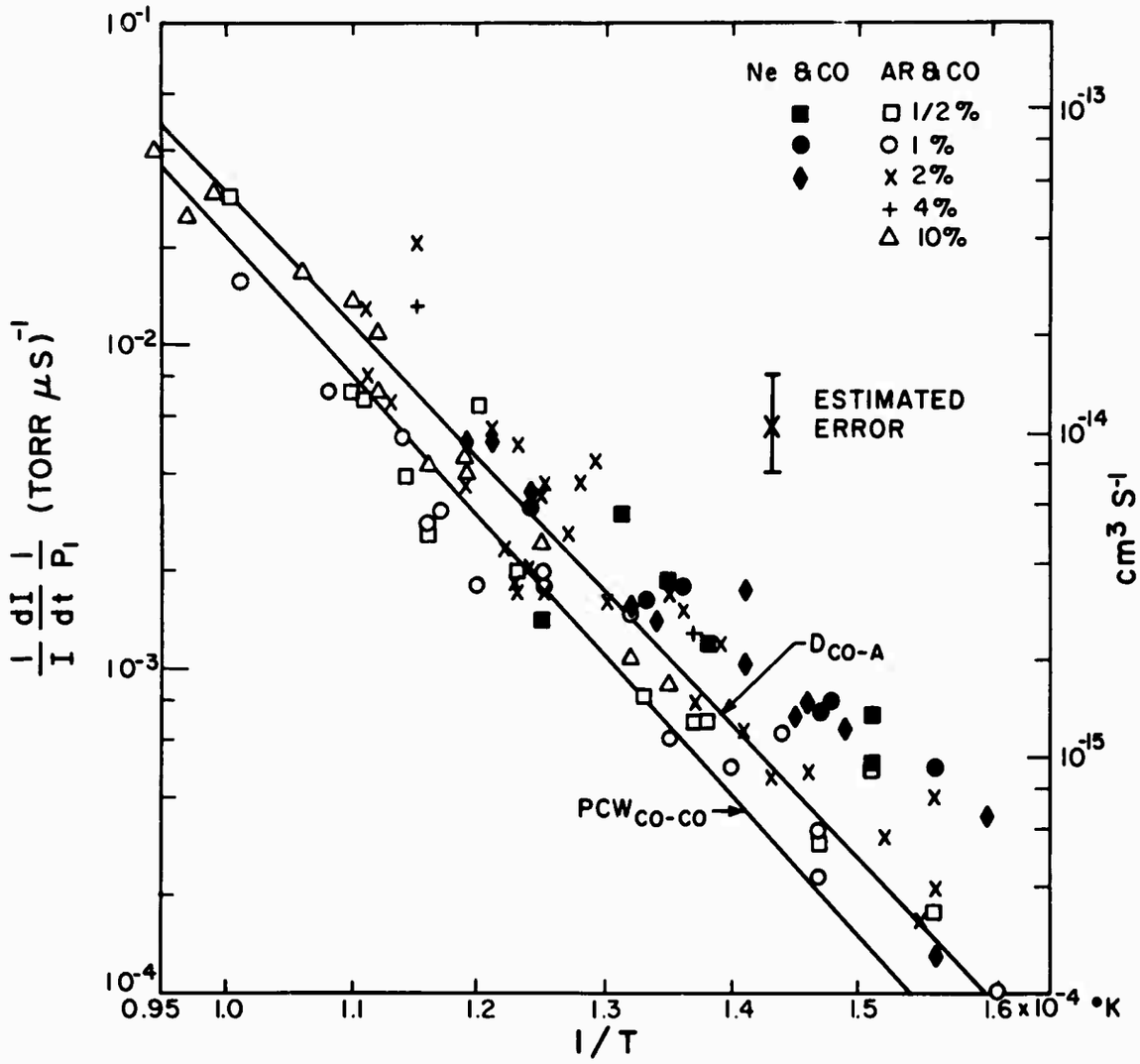

Fig. 7 CO dissociation rates obtained from the final slopes.

A5189

C_2 Behavior

Of the possible products of shuffle reactions only C_2 was observed. In the photographic spectra taken, both $C_2\,^1\Sigma$ and $C_2\,^3\Pi$ were identified. The photoelectric studies concentrated entirely on the C_2 Swan bands ($^3\Pi \rightarrow {}^3\Pi$). While in reaction (2) it is reasonable to suppose the C and O atoms to be in their ^3P ground states, and CO in the $X^1\Sigma$ state, it is not obvious what state the C_2 will be in. The $X^1\Sigma$ and $X^3\Pi$ states are very close in energy and in the data reduction it has been assumed that full equilibrium exists between these two states. It was also assumed that the observed emission was in local equilibrium and absolute concentrations of C_2 were obtained by the use of a previously obtained f number.[20] In some of the experiments at low CO concentrations and low initial pressure, it is possible that the radiation will be collision limited and so the concentration deduced from emission will be lower than the true value. At most this effect will not exceed a factor of two.

The emission in the Swan bands showed a gradually increasing slope forming a toe at the shock front. Within a few microseconds the rise became effectively linear. The radiation went through a peak, which occurred after the end of the incubation time and then declined with the same profile as the CO indicating that the C_2 and CO were in steady state. Towards the end of the dissociation the C_2 is a more useful observable than the infrared which becomes dominated by Bremstrahlung.

The linear part of the C_2 rise was measured for a range of conditions and the results given in Fig. 8. Using the mechanism of reactions (1), (2) and (4), putting C_2 in steady state and neglecting back reactions it may be estimated that $d[C_2]/dt \approx 2k_1k_2[CO]^2/k_4$. The use of any other power of

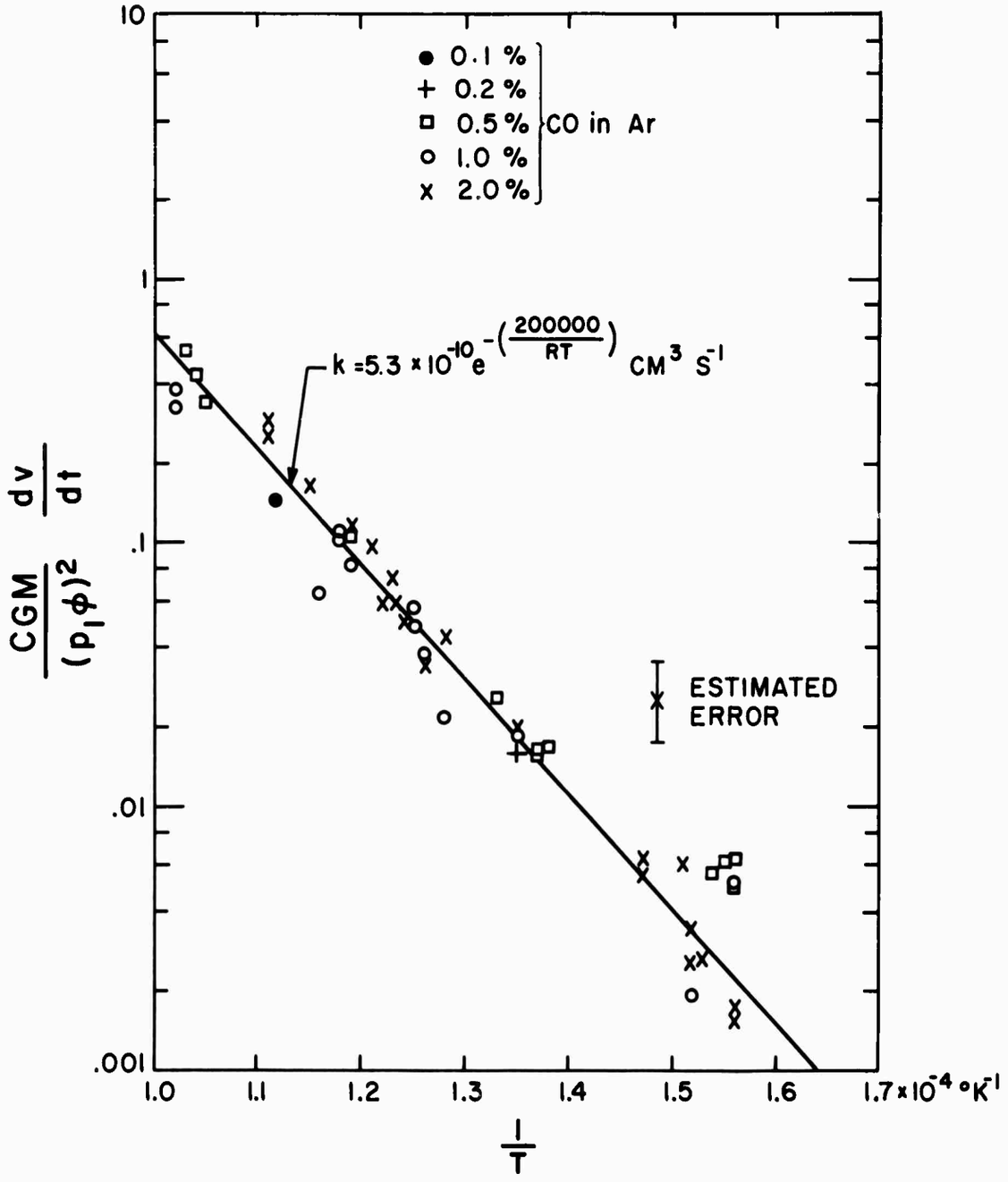

Fig. 8 C_2 formation rate during incubation time. The ordinate is in mV/μsec, C is a calibration factor, G is the solid angle subtended by the gas at the spectrometer, M^{-1} is the fraction of C_2 molecules radiating in the band pass. By the use of the f number in Ref. 20, d $[C_2]$/dt (particles/cc sec) is given by 3.15 x 10^{17} x ordinate for $p_1 = 1$ torr, $\phi = 1.0$. Figures 9 through 16 present comparisons between calculations and experiment. All times are given in laboratory coordinates.

A9091

[CO]gave much greater scatter of the points. The activation energy found, 200 k cal/mole, is consistent with the ratio $k_1 k_2 / k_4$. The reaction

$$CO + CO \rightleftarrows C_2 + O_2 \qquad (6)$$

has an endothermicity of 250 K cal/mole and if an estimate of 0.28 $(D_{O_2} + D_{C_2})$[21] is added to this, a total activation energy of about 320 K cal/mole is expected. By the use of pre-exponential factors in the rate expression, it is possible to fit the slope with the form $k \propto (E/RT)^n \exp(-E/RT)$ with E = 320 K cal/mole and n = 9. For a collision of two CO molecules the greatest value of n which is classically allowed is 4 and so the above reaction cannot contribute to the C_2 formation in a major way.

The other shuffle reaction, forming O_2 via reaction (3) was not directly observed. Its effect was deduced from some experiments in which O_2 was added to the CO mixture. With equal amounts of O_2 and CO diluted with 98% Ar, there was an initial reaction rate almost obliterating the incubation time since there was no point at which the slope obviously changed, Fig. 16a. These experiments will be more fully discussed in the section on computation.

Other Reactions

It has already been mentioned that many reactions may be written down for this system. For instance

$$CO + CO \rightarrow C_2O + O \qquad (7)$$

(C_2O has recently been discovered as a result of the action of C atoms on CO in a matrix)[22] and its analogue

$$CO + CO \rightarrow CO_2 + C \qquad (8)$$

are also candidates for the removal of CO. If the latter reaction should be the producer of carbon atoms required for reaction (2) rather than reaction (1), then the incubation time parameter should be $\tau\ p\ \phi$ rather than $\tau\ p\ \phi^{1/2}$ and the activation energy of the plots of Fig. 4 should be around 65 K cal/mole, neither of which is in accord with the experiments. These considerations indicate that the above reactions are not dominant. Such is the scatter of data that it cannot be shown whether or not such reactions do occur to a minor extent.

C_2O may also participate in the reaction scheme by producing the C_2 by a reaction such as

$$C_2O + C \rightarrow C_2 + CO \qquad (9)$$

and if the main removal of C_2O is the decomposition

$$C_2O + M \rightarrow CO + C + M \qquad (10)$$

The heat of dissociation of reaction (10) is not known for certain, but has been estimated[23] as 44 K cal/mole. This value is probably low but not of great consequence for the following analysis. The steady state analysis already applied to the formation of C_2 from the reactions (1), (2) and (4) gives

$$[C_2] \approx \frac{k_2 [CO][C]}{k_4 [M]} \quad \text{and} \quad \dot{[C_2]} \approx \frac{2k_1 k_2 [CO]^2}{k_4}$$

a similar analysis, putting both $[C_2]$ and $[C_2O]$ in steady state, using reaction (7) and (10) gives

$$[C_2O] = \frac{k_7 [CO]^2}{k_{10}[M]}$$

and

$$[C_2] = \frac{k_9 [C_2O][C]}{k_4 [M]} \; ; \text{ thus } [C_2] = \frac{k_7 [CO]^2 [C]}{k_4 k_{10} [M]^2}$$

and if the C atoms are produced mainly by reaction (8) we obtain

$$[\dot{C}_2]_A = \frac{k_7 k_8 [CO]^4}{k_4 k_{10} [M]^2}$$

and if (1) is the reaction to produce carbon atoms,

$$[\dot{C}_2]_B = \frac{k_1 k_7 [CO]^3}{k_4 k_{10} [M]}$$

Neither of these expressions fits the data of Fig. 8, either in the concentration or slope dependences, giving respectively 56 and 181 K cal/mole for the activation energy. By adjusting the heat of reaction of 10 to 84 K cal/mole, a value which is probably too high, the slope may be made to fit, but the concentration dependence remains at variance with the data.

For these reasons, it is not felt that reactions (7) through (10) have any importance in the high temperature dissociation of carbon monoxide. Because of the unimportance of O_2 in the dissociation of CO, the possible triatomic reactions leading to it may be ignored.

Impurity Effects

It has been commented earlier that nitrogen impurity in the gas gave rise to CN radiation. It is probable that CN too will be formed in shuffle

reactions and might thus act as another intermediate in the CO dissociation path. Nitrogen impurity added in amounts up to 5% of the carbon monoxide content has no observable effect on the second rate, neither did a similar addition of oxygen or of carbon tetrachloride. The effect of impurity addition on the initial slope was also not significant in the case of nitrogen and oxygen but the carbon tetrachloride experiments did show about a factor of two enhancement of the rate at temperatures below 8000°K. There is very little data above that temperature.

COMPUTER STUDIES

Of the reactions mentioned as probably important, i.e., (1) through (5), only one, the oxygen dissociation rate, has been measured. All of the others are unknown. Parametric computer studies were undertaken to find a plausible, self-consistent set of rate constants which will predict both the CO and C_2 histories for a wide range of conditions. The experiments all lie in the range of temperature between about 6000°K below which they are too slow and shock attenuation effects become troublesome and 10,000°K where the experimental time is very short and ionization gives spurious signals.

Because of the complexity of the reaction, it was not considered meaningful to try to establish the temperature variation of the backward rate constants (all rates will be given in the backward direction as written, i.e., in the exothermic direction, by relating the forward and backward rates through the equilibrium constant). Rather, the attempt will be made to establish the rates to a close order of magnitude in this temperature range.

Two different programs have been used. One is based on the steady state approximation for the intermediate species C_2, O_2, the rate of change of whose concentration is very much less than that of C, O, or CO.

The final equilibrium conditions were found from an equilibrium program due to Los Alamos Laboratory, neglecting ionization, thus the final degree of dissociation was found. The reaction was divided into 100 equal steps of dissociation and the average concentration of each of the species found at each step. An estimated set of rate constants was used and thus the time required for each given change in α, the degree of dissociation was found. A running integral of the time was maintained, converted to lab time via the relation $\Delta t_\ell = \Delta t_g / \overline{\rho}$, where $\overline{\rho}$ is the average density ratio across the shock at point of interest.

Boundary Layer

Many of the experiments were followed well into the test gas (laboratory times > 20 μ s). In these experiments boundary layer growth is important. This leads to four main effects. The boundary layer reduces the path length through the hot gas and sheaths this hot core with cold gas. For the CO infrared and C_2 visible radiation, this will not affect the radiation as seriously as the other concomitants of the boundary layer which comprise a decrease in particle velocity with respect to the shock front, leading to an increase of enthalpy of a particle behind the shock and to an increase in particle time which is now given by $t_g = t_\ell \, \overline{\rho} \, F(t)$ where $F(t)$ is greater than unity. These effects will, in the absence of corrections, give rise to deduced reaction rates which are too great. Towards the end of the test gas the effect in time alone can be a factor of about 5. Pari passu with the boundary layer growth a deceleration of the shock occurs.

This also leads to progressively higher enthalpy behind the shock. Mirels[24] has given expressions applicable to the center stream line for the time and particle velocity transformation.

$$\frac{U_e}{U_{eo}} = 1 - \left(\frac{\ell}{\ell_m}\right)^{1/2}$$

which gives

$$-\frac{x_s}{2\rho_2/\rho_1 \cdot \ell_m} = \ell n\left(1 - \frac{\ell}{\ell_m}\right)^{1/2} + \left(\frac{\ell}{\ell_m}\right)^{1/2}$$

where U_e is particle velocity with respect to the shock, U_{eo} is the velocity at the shock front. ℓ is the distance behind the shock front, ℓ_m is the maximum length of the test slug and is obtained from Mirels' curves assuming a laminar boundary layer. $x_s = t_g U_s$ and $\ell = t_\ell U_s$ where U_s is the shock velocity. The shock attenuation effect on enthalpy was estimated by assuming a linear enthalpy rise behind the shock with distance. The shock velocity corresponding with the gas at the contact face was estimated from the velocity measurements made along the tube. We thus obtain

$\Delta H_e = 1/2\, M(U_s^2 - U_e^2)$, M is the molecular weight

$U_e = U_s + \ell/\ell_x(U_x - U_s)$, x denotes the contact surface.

In reality, the situation is more complicated, since wave interactions are involved and not just enthalpy addition. These effects have never been properly treated and lie beyond the scope of these studies.

The Avco stream tube program[3] has also been used to study the reaction system, using as input the initial estimates obtained from the steady state program.

As is to be expected, the effect of the boundary layer increases progressively with distance behind the shock and about halfway through the test gas the correction is about a factor of two. Since the correction is somewhat uncertain itself, there is little value in analyzing the data beyond this point. The effect of the boundary layer on the incubation is within the experimental error of measuring the time.

Reaction Rates (Estimates from Data)

Since only the rate of reaction (5) is known, it is required to find the rates of the other four. In order to do this it is necessary to make estimates of what is likely to be the upper bounds of the rates so that the computations are not forced to fit the data by a set of unrealistic assumptions. As a starting point, the estimates made from the experiments were used. It has already been shown that $k_4^- \approx 10\, k_1^-$ and in conjunction with the C_2 rise experiments, from which $[C_2] / [CO]^2 = 1.9 \times 10^{-15}$ at 8000°K, k_2^- may be estimated, since $1.9 \times 10^{-15} = 2k_1^- k_2^- K_2^2 / k_4^-$ from the expression given earlier. Thus $k_2^- \approx 3 \times 10^{-10}$.

The initial slope measurements gave $k_1^- \approx 4 \times 10^{-34}$ and the second slope measurements of the CO traces yield $k_4^- \approx 4 \times 10^{-33}$ at 8000°K neglecting the contribution of k_1^- and taking $[C_2] \approx 1/2\, K_2 [CO]$.

Because of the approximations involved in deriving the various kinetic expressions, it is not expected that the rates obtained from them are accurate. The initial input to the calculations was taken as

$k_1^- = 10^{-34}$, $k_2^- = 3 \times 10^{-10}$, $k_4^- = 3 \times 10^{-33}$ and thereafter these rates were adjusted to obtain as good fits as possible over a range of experiments. Samples of data, along with the computer analysis, are shown in Figs. 9-16; these are discussed in appropriate places below, but details are given in the figure captions.

By assuming arbitrary values for k_3^- it was found that reaction (3) had no perceptible effect unless $k_3^- > 10^{-8}$. This is an unreasonably high value and so the participation of O_2 as an intermediate was ignored in CO and noble gas experiments. In this determination attention was paid to both the C_2 and CO profiles. One of the main difficulties was experienced in the matching of the CO profiles. It has already been noted the Bremsstrahlung probably obscures the initial decay of the CO and affects the observed later decay as well. The rising tail of the infrared signal in a run such as shown in Fig. 10a was rather arbitrarily extrapolated linearly back towards the shock front and the CO signal taken as the difference between this line rather than the base line and the trace. Figure 10b also shows the CO data reduced with respect to the base line. The difference is greater than the uncertainty of reading the trace which is also indicated in Fig. 9(d). It is clear that in future work the Bremsstrahlung should be measured independently in order to allow for its effect on the CO channel.

While unimportant in CO and noble gas mixtures, reaction (3) is of importance when much oxygen is present.

It will be noted that there are two major discrepancies in the calculated and observed C_2 histories. In the 10% CO mixtures the C_2 level computed was higher than that observed although multiplying the experimental value for the C_2 by a factor of two brought them into excellent agreement, Fig. 14b. It is not known why this is so, but absolute intensity work does

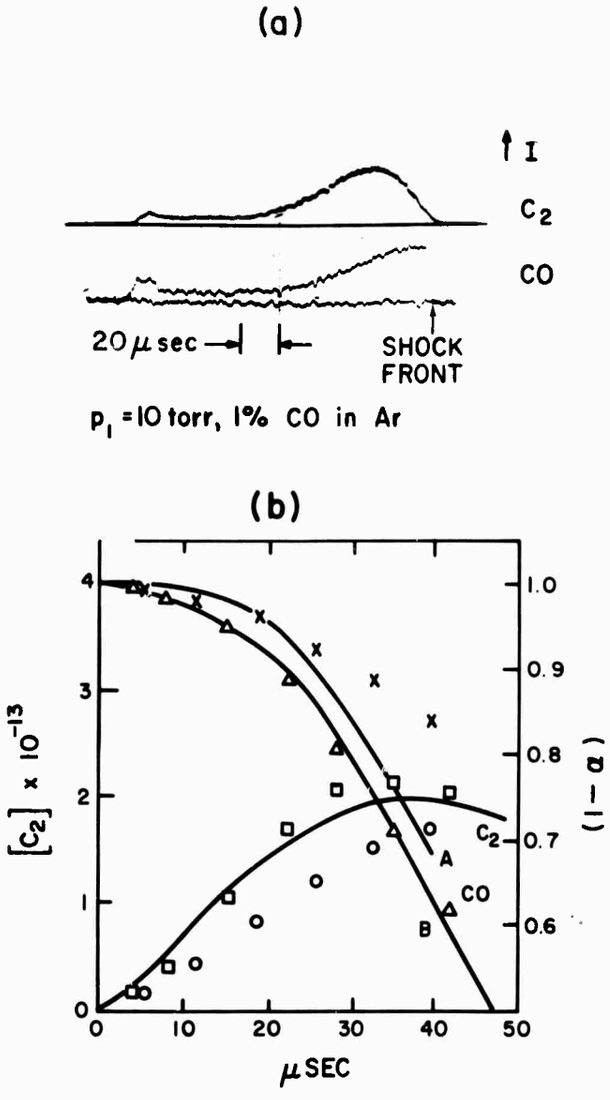

Fig. 9a Experimental data: shock speed = 2.86 mm/μsec; T at front = 7600°K. Because of non-coincidence of optical beams, the traces do not rise at the same part of the oscillograph sweep.

b Analysis of (a): The solid lines are smoothed experimental data. For CO two lines are given, marked A and B. A refers to the trace height above the base line and B is obtained making an allowance for Bremsstrahlung which is assumed to grow linearly from the shock front. α is the degreee of dissociation of the CO. The points coded with open squares, □ for C_2 and open upright triangles, Δ for CO, always refer to the rates given in Table 1. Open circles, O for C_2 and crosses X for CO, refer to a calculation made with Table 1 rates but ignoring the boundary layer.

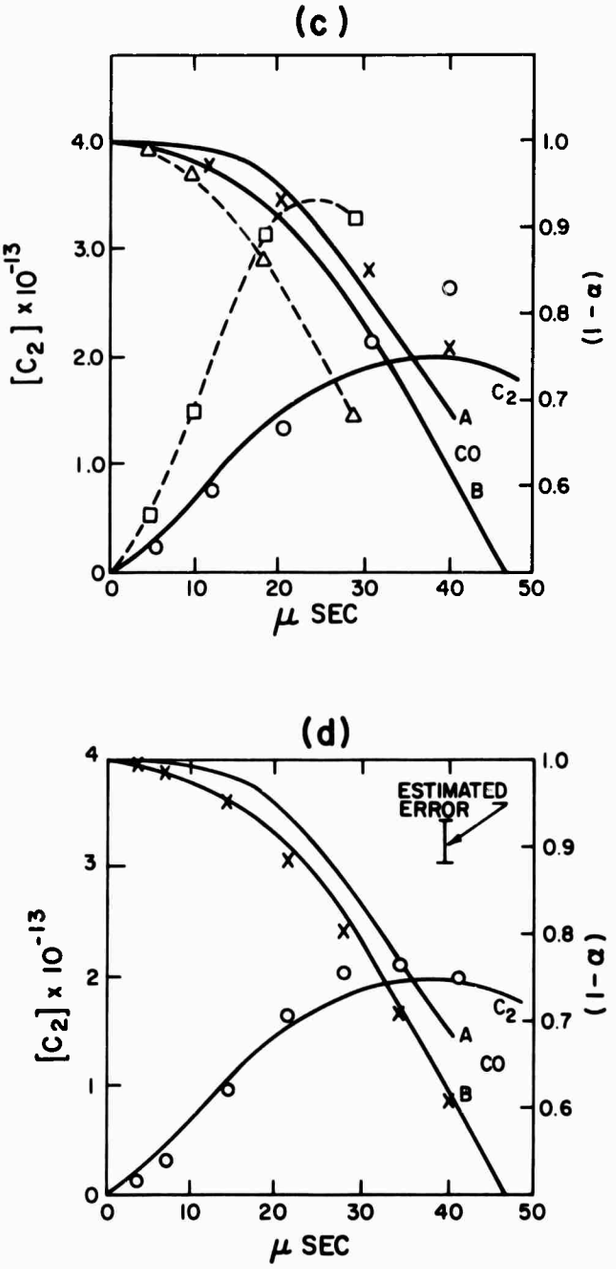

Fig. 9c A second analysis of (a): The steady state approximation was used for the calculation and boundary layer effects included. As before □ and Δ refer to C_2 and CO using Table 1 rates, ○ and × were obtained putting $k_1^- = 2 \times 10^{-34}$, $k_2^- = 2 \times 10^{-10}$, $k_4^- = 2 \times 10^{-33}$.

d A third analysis of (a): The integration of the rate equations allowing for boundary layer was used. ○ and X were obtained putting $k_1^- = 2 \times 10^{-34}$, $k_2^- = 4 \times 10^{-10}$, $k_4^- = 2 \times 10^{-33}$, $k_{13}^- = 2 \times 10^{-9}$, $k_{14}^- = 2 \times 10^{-33}$.

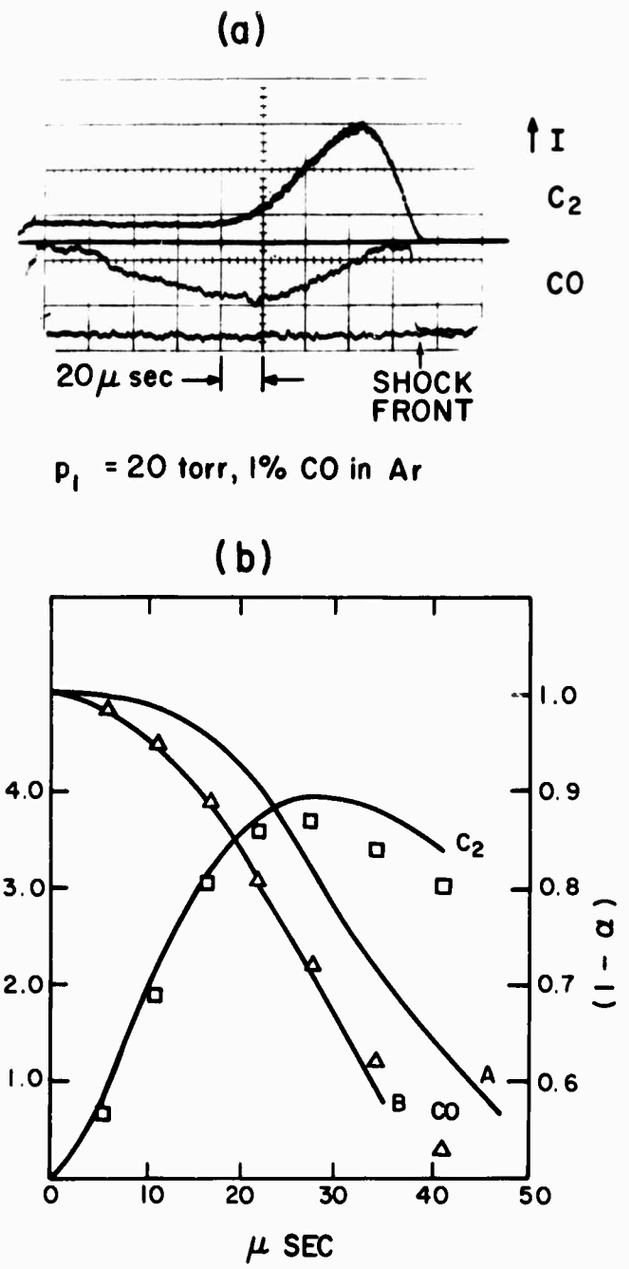

Fig. 10a Experimental data. Shock speed 2.82 mm/μsec, T at front = 7400°K. The Bremsstrahlung is very evident in the CO channel 80 μsec behind the shock front.

b Analysis of (a) using rates from Table 1.

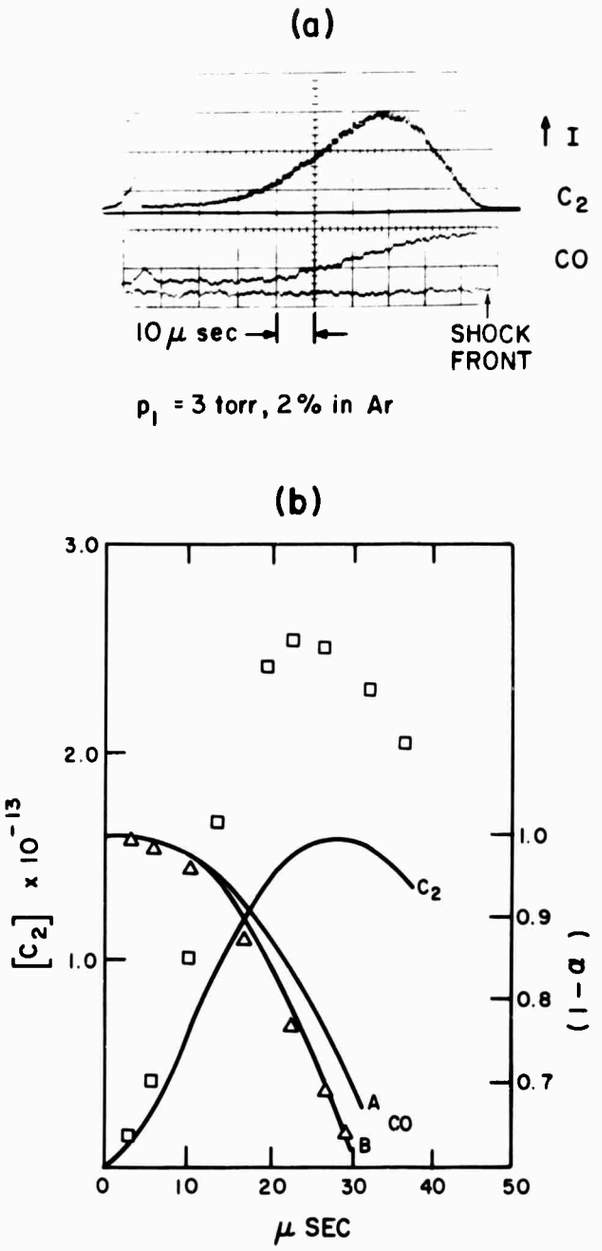

Fig. 11a Experimental data. Shock speed = 3.00 mm/μsec, T at front = 8300°K.

b Analysis of (a).

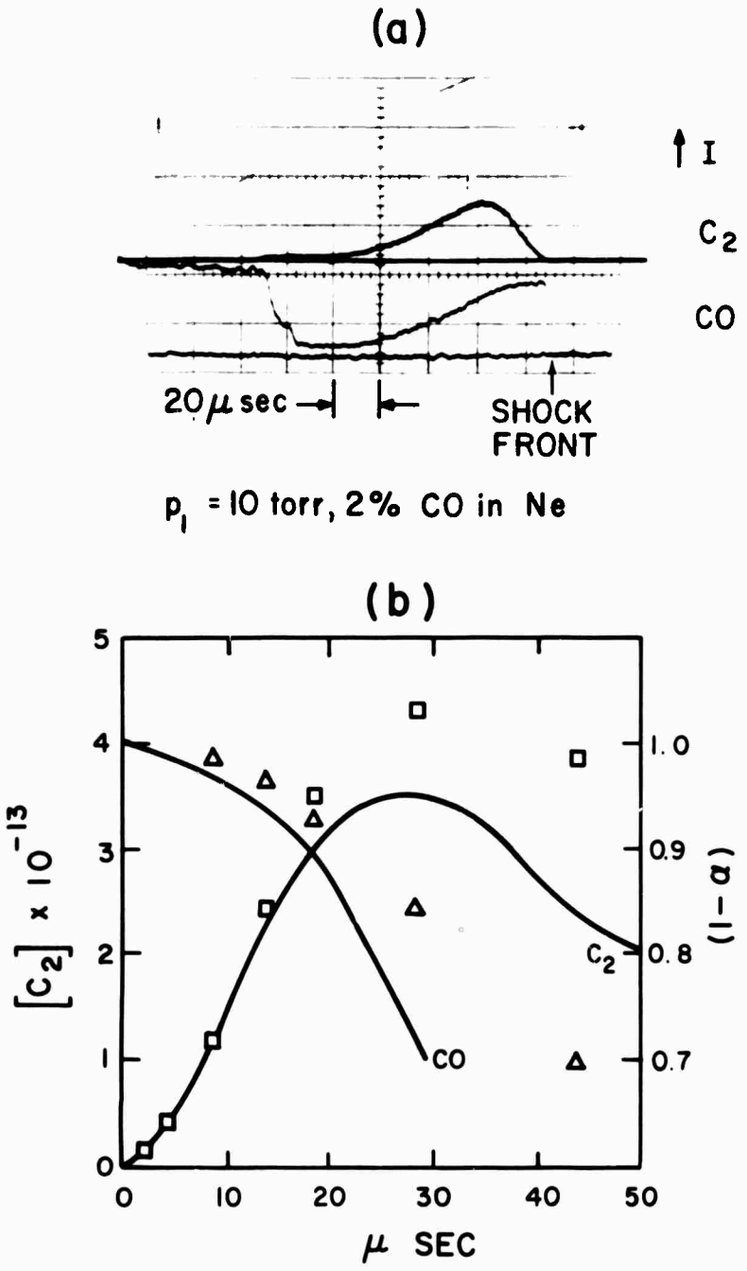

Fig. 12a Experimental data. Shock speed = 3.94 mm/μsec, T at front = 7300°K

b Analysis of (a). This run was combustion driven and the derivation of the calculated and observed profiles at some distance behind the front is due to the severe attenuation which occurred.

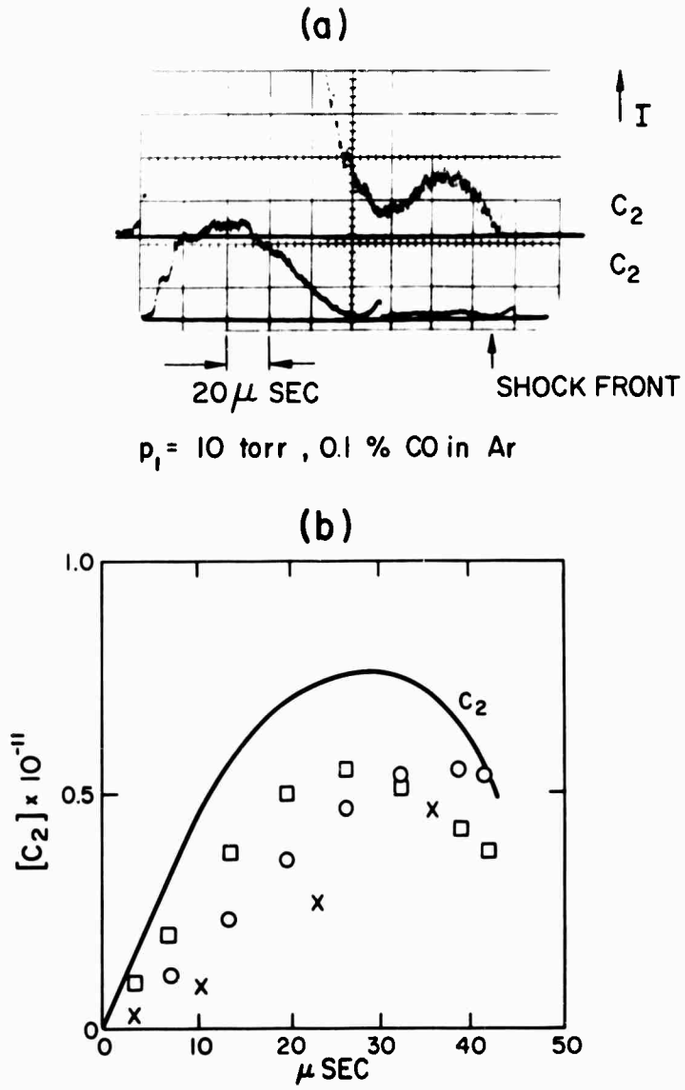

Fig. 13a Experimental data. Shock speed = 3.08 mm/μsec, T at front = 8800°K. Both traces are of C_2. The lower is at lower amplification than the upper and has signals generated from heat transfer gauges impressed upon it. On the upper trace there is a slight overshoot at the shock front probably due to a trace of impurity. The marked rise occurring about 60 μsec after the shock front is due to the onset of ionization.

b Analysis of (a). Three computations were made. The open squares, □, refer as before to rates in Table 1. The open circles ○, have the same rates but $k_1^- = 1 \times 10^{-34}$ and the crosses, X, $k_1^- = 0.5 \times 10^{-34}$.

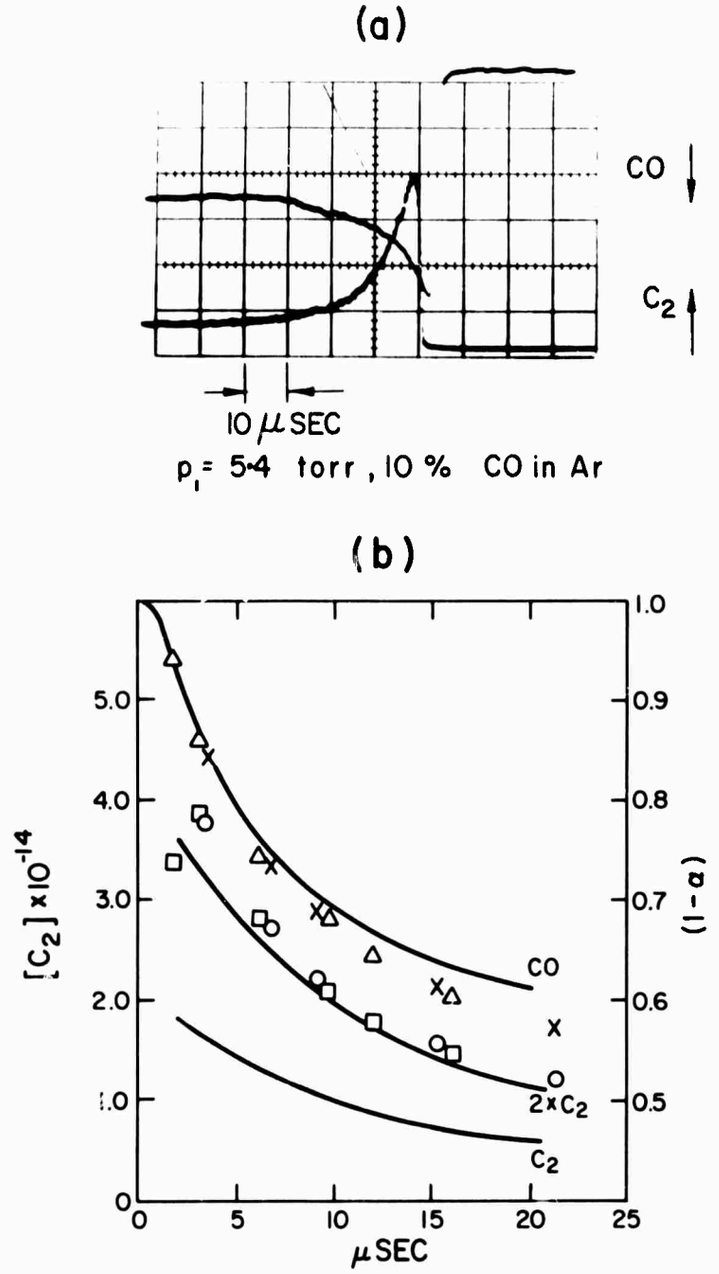

Fig. 14a Experimental data. Shock speed = 3.26 mm/μsec. T at front = 9000°K. Because of the way the amplifiers were connected, the traces in this run go in opposite directions.

b Analysis of (a). The open circles for C_2 and crosses for CO were obtained with $k_1^- = 1 \times 10^{-34}$. Open squares for C_2 and triangles for CO with Table 1 data.

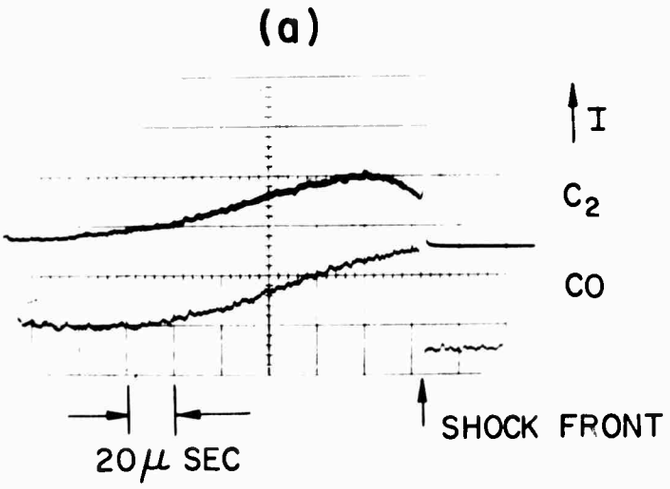

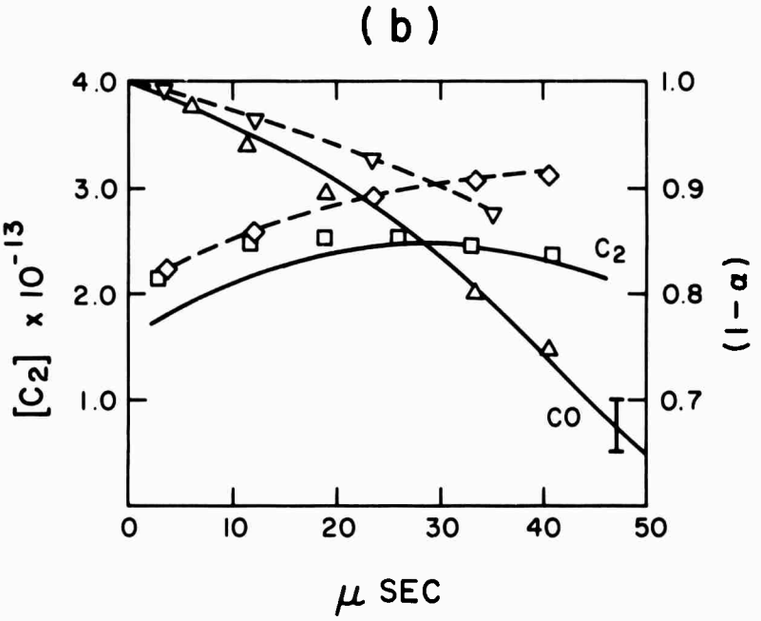

Fig. 15a Experimental data. Shock speed = 2.76 mm/μsec, T at front = 7000°K. The C_2 channel shows a strong overshoot which decays within 4 μsec of the shock front. This is due to the dissociation of the CCl_4 added.

b Analysis of (a). The open diamonds for C_2, and inverted triangles for CO, ∇, were obtained from the steady state calculations with Table 1 values except $k_2^- = 2 \times 10^{-10}$ and $k_4^- = 2 \times 10^{-33}$.

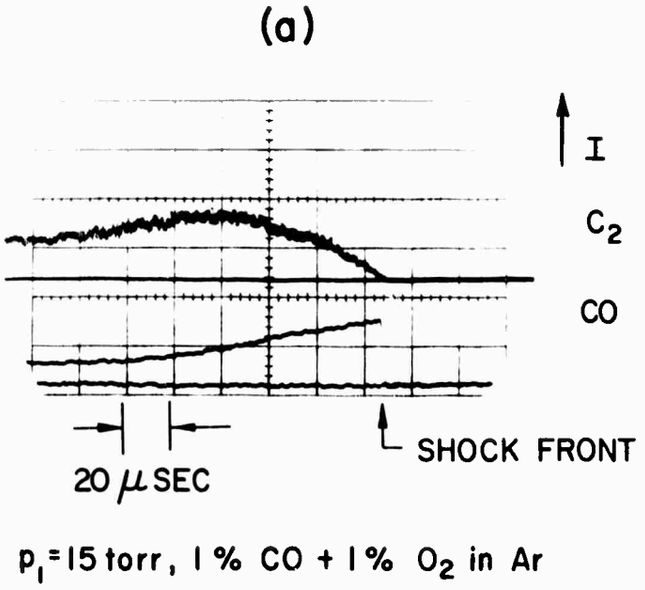

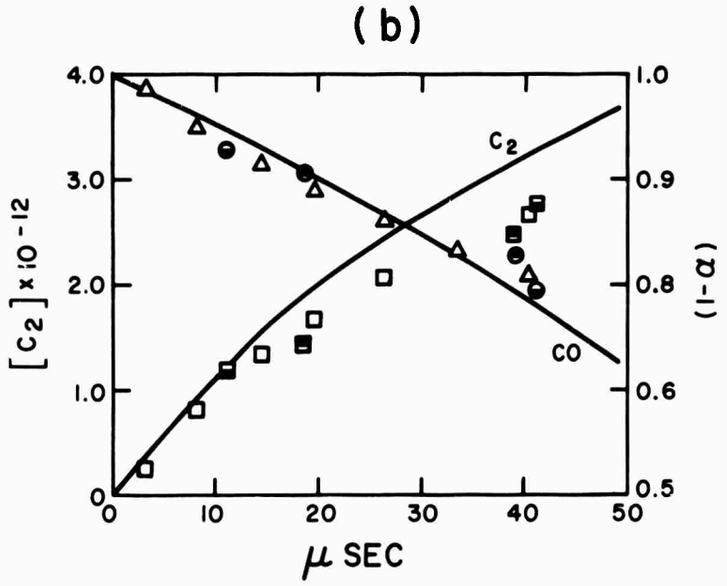

Fig. 16a Experimental data. Shock speed = 2.80 mm/μsec, T front = 7200°K.

b Analysis of (a). In this experiment the O_2 was dissociated within 1 μsec of the shock front. These calculations are presented and Δ refer to Table 1 rates. The half shaded squares ◻ and circles ○ at the top have the same rates except $k_3^- = 3 \times 10^{-10}$ and those shaded at the bottom, ◻ and ○ have $k_3^- = 7 \times 10^{-10}$.

tend to have scatter of factors of two and since the shape of the profile is good, the failure to match the concentration exactly is not thought significant.

The possible contribution to the C_2 channel by CO triplet radiation is probably small. It was estimated from the photographs of the spectra that the CO radiation if it occurs in the visible in at least an order of magnitude less intense than the C_2 since it was never observed. It is possible that there is a small component of triplet band radiation ($d^3\Delta \rightarrow a^3\Pi$). The oscillator strength of this system is not known and neither are the mechanisms, if they exist, for the production of the excited CO. Arguments made earlier in this paper indicate that the most likely collision partner is CO itself, and in this case the CO^* will rise proportional to $[CO]^2$ and time until about 3 μs in laboratory coordinates. The computed C_2 also rises proportional to $[CO]^2$ and time, once an initial time has elapsed. A decrease in the [CO] concentration should allow the effect to be sorted out, since the CO^* will always rise in a time of order 3 μ sec. Unfortunately, the noise also increases and mixtures of less than 1/2% CO were not investigated. The results never indicated that CO^* might contribute appreciably to the C_2 channel signal.

The Effect of Added Oxygen

The analysis shown in Fig. 16b of a 1% CO plus 1% O_2 plus 98% Ar indicates that a large amount of oxygen speeds up the reaction particularly near the shock front. In this experiment the O_2 will be dissociated in the order of the resolution time of the experiment. Although a pathway via CO^* could be contemplated assuming $CO + O \rightarrow CO^* + O$ to be rather faster than $CO + CO \rightarrow CO^* + CO$ this would require O to be more effective than CO which already has a close to gas kinetic cross section. This is improbable.

The observations are explained by reaction (3) followed by (5). Since the rate of (5) is already known, only the rate of (3) is to be found. A good fit is obtained with $k_3^- = 5 \times 10^{-10}$ cm^3 s^{-1}, although the computations are not particularly sensitive to 50% changes in this value, Fig. 16b.

Assuming the mechanism of formation of C_2 already given, a check was made by the replacement of 5% of the CO by O_2, in a mixture with 99% argon at 6900°K it was found that the C_2 slope was a factor of three lower than that expected from the relation in Fig. 8. Under these conditions the backwards reaction (2) will be important and the result indicates that $k_2^-/k_3^- = 2 \times 10^{23}$, a value quite consistent with the rates obtained from other expressions. Such experiments further indicate the appropriateness of the mechanism given for C_2 formation.

Possibility of CO^* Being Important

If the arguments based on Ref. 15 are invalid, CO^* could also be involved in the mechanism of the overall reaction. In the absence of independent rates for reactions (2) and (4), it is impossible to do more than find the limits of rates for a mechanism based on CO^*, and for completeness' sake, computer runs were also made assuming that the incubation was due to CO^*, formed by the reaction

$$CO + C \rightarrow CO^* + C \qquad (13)$$

and followed by

$$CO^* + M \rightarrow C + O + M \qquad (14)$$

and it was required that $k_{13}^- = 2 \times 10^{-9}$ and $k_{14}^- = 2 \times 10^{-33}$, Fig. 9d. This rate of (13) is inordinately high and the true rate is almost certainly lower. Further experimental work will be necessary before reactions (13) and (14)

can be either eliminated or included with any certainty. Because of their possibility, the rates found for (2) and (4) must also be considered as upper limits.

Steady State Approximation

The steady state solutions obtained are also presented in Figs. 9c and 15b. It will be noted that they give quite a fair representation and are not significantly different from the full integration procedure which uses more computer time. Although they have been in use for many years, steady state approximations are frequently considered to be badly in error. In this system at least, this is not true. Its advantage lies with those without access to computers. For instance, even taking wide intervals, the steady state method does not lead to oscillating solutions and hand calculations are readily made. The results are also presented to justify the use of steady state arguments used earlier. It is evident that while the magnitudes of reaction rates so obtained may be in error, the approximation gives the right form of the result.

SUMMARY AND CONCLUSIONS

The dissociation of carbon monoxide has been investigated by observing its infrared and visible radiation. The reaction is not a simple one and is best explained as a chain reaction with C_2 as the important intermediate. The rates which best fit the data based on computed histories including boundary layer buildup but not attenuation are:

TABLE 1

Reaction	Rate Constant
$C + O + M \rightarrow CO(X^1\Sigma) + M$,	$= 2 \times 10^{-34}$ cm^6 s^{-1}
$C_2 + O \rightarrow CO(X^1\Sigma) + C$,	$= 6 \times 10^{-10}$ cm^3 s^{-1}

$O_2 + C \rightarrow CO(X^1\Sigma) + O$, $= 5 \times 10^{-10}$ cm^3 s^{-1}

$C + C + M \rightarrow C_2 + M$, $= 3 \times 10^{-33}$ cm^6 s^{-1}

These rates are upper bounds which may need to be modified downwards if alternate reactions prove to be important. The uncertainties are estimated as $\pm$ 50%.

ACKNOWLEDGMENTS

The author is grateful for the assistance given by Mr. P. MacLean and Mrs. I. Justh with the computations and Mr. R. M. McMillan with the experiments.

REFERENCES

1. Camac, M., and Vaughan, A., J.C.P. 34, 640 (1961).

2. Jacobs, T.A., and Giedt, R.R., J.C.P. 39, 749 (1963) and Hiraoka, H., and Hardwick, R., J.C.P. 36, 1715 (1962).

3. Keck, J.C., and Carrier, G., J.C.P. 43, 2284 (1965).

4. Camac, M., Feinberg, R., and Teare, J. D., Avco Everett Research Laboratory Research Report 245 (1966).

5. Malkmus, W., and Thomson, A., J.Q.S.R.T. 2, 17 (1961).

6. Hooker, W.J., and Milikan, R.C., J.C.P. 38, 214 (1963).

7. Fairbairn, A.R., Avco Everett Research Laboratory Research Report 299.

8. Duff, R.E. and Davidson, N., J.C.P. 31, 1018 (1959).

9. Sultzmann, K.G.P., Myers, B.F. and Bartle, E.R., J.C.P. 42, 3969 (1965).

10. Tobias, I., Fallon, R.J., and Vanderslice, J.T., J.C.P. 33, 1638 (1960).

11. Brau, C.A., private communication (1966).

12. Davies, W.O., I.I.T.R.I. -T 200-8, I.I.T. Research Institute Chicago (1964).

13. Tanaka, Y., Jursa, A.S. and LeBlanc, F., J.C.P. 26, 862 (1957).

14. Hesser, J.E., and Dressler, K., Ap. J. 142, 389 (1965).

15. Hansche, G.E., Phys. Rev. 57, 289 (1940).

16. Fairbairn, A.R., J.C.P. 48, (1968).

17. Petschek, H. and Byron, S.R., Annals of Phys. 1, 270 (1957).

18. Taylor, R.L. and Caledonia, G., 5th Conference on Electronic and Atomic Collisions, Leningrad (1967).

19. Presley, L. L., Chackerian, C. and Watson, R., AIAA Paper 66-518 (1966).

20. Fairbairn, A.R., J.Q.S.R.T. 6, 325 (1966).

21. Hirshfelder, J.O., J. Chem. Phys. 9, 645 (1941); see also Bar-Nun, A., and Lifshitz, A., J. Chem. Phys. 47, 2878 (1967).

22. Jacox, M.E., Milligan, D.E., Moll, N.G. and Thompson, W.E., J.C.P. 43, 3734 (1965).

23. von Weyssenhoff, H., Dondes, S. and Harteck, P., J.A.C.S. 84, 1526 (1962).

24. Mirels, H., Phys. Fluids 6, 1201 (1963).

UNCLASSIFIED
Security Classification

DOCUMENT CONTROL DATA - R&D

(Security classification of title, body of abstract and indexing annotation must be entered when the overall report is classified)

1 ORIGINATING ACTIVITY (Corporate author)
Avco Everett Research Laboratory
2385 Revere Beach Parkway
Everett, Massachusetts

2a REPORT SECURITY CLASSIFICATION
Unclassified

2b GROUP

3 REPORT TITLE
The Dissociation of CO

4 DESCRIPTIVE NOTES (Type of report and inclusive dates)
Research Report 305

5 AUTHOR(S) (Last name, first name, initial)
Fairbairn, A. R.

6 REPORT DATE	7a TOTAL NO OF PAGES	7b NO OF REFS
December 1968	50	24

8a CONTRACT OR GRANT NO.
Contracts AF 04(694)-690
AF 04(694)-983
F04701-68-C-0036

b PROJECT NO

c

d

9a ORIGINATOR'S REPORT NUMBER(S)
Research Report 305

9b OTHER REPORT NO(S) (Any other numbers that may be assigned this report)
SAMSO-TR-68-398

10 AVAILABILITY LIMITATION NOTICES
Distribution of this document is unlimited. This indicates document has been cleared for public release by competent authority.

11 SUPPLEMENTARY NOTES

12 SPONSORING MILITARY ACTIVITY Advanced Research Projects Agency, Department of Defense, ARPA Order #1092 and Space and Missile Systems Organization, Air Force Systems Command, Deputy for Re-entry Systems (SMY), Norton Air Force Base, California 92409.

13 ABSTRACT

The dissociation of carbon monoxide diluted with noble gases has been studied in a shock tube. The reaction is complex and appears to be a chain with C_2 as the important intermediate. At temperatures around 8000°K, the reaction rates found to be consistent with the data are $O + C + M \rightarrow CO + M$, $k_r = 2 \times 10^{-34}$ cm^6 sec^{-1}; $C + C + M \rightarrow C_2 + M$, $k_r = 3 \times 10^{-33}$ cm^6 sec^{-1}; $C_2 + O \rightarrow CO + C$, $k = 6 \times 10^{-10}$ cm^3 sec^{-1}; and $O_2 + C \rightarrow CO + O$, $k = 5 \times 10^{-10}$ cm^3 sec^{-1}.

DD FORM 1 JAN 64 1473

UNCLASSIFIED
Security Classification

KEY WORDS	LINK A		LINK B		LINK C	
	ROLE	WT	ROLE	WT	ROLE	WT
1. CO						
2. Dissociation rate						
3. Mechanism of reaction						
4. Shock tubes						
5. High temperature						
6. Formation of C_2						
7. Infrared radiation from CO						
8. Visible radiation from CO						
9. Atomic carbon radiation from CO						

INSTRUCTIONS

1. ORIGINATING ACTIVITY: Enter the name and address of the contractor, subcontractor, grantee, Department of Defense activity or other organization *(corporate author)* issuing the report.

2a. REPORT SECURITY CLASSIFICATION: Enter the overall security classification of the report. Indicate whether "Restricted Data" is included. Marking is to be in accordance with appropriate security regulations.

2b. GROUP: Automatic downgrading is specified in DoD Directive 5200.10 and Armed Forces Industrial Manual. Enter the group number. Also, when applicable, show that optional markings have been used for Group 3 and Group 4 as authorized.

3. REPORT TITLE: Enter the complete report title in all capital letters. Titles in all cases should be unclassified. If a meaningful title cannot be selected without classification, show title classification in all capitals in parenthesis immediately following the title.

4. DESCRIPTIVE NOTES: If appropriate, enter the type of report, e.g., interim, progress, summary, annual, or final. Give the inclusive dates when a specific reporting period is covered.

5. AUTHOR(S): Enter the name(s) of author(s) as shown on or in the report. Enter last name, first name, middle initial. If military, show rank and branch of service. The name of the principal author is an absolute minimum requirement.

6. REPORT DATE: Enter the date of the report as day, month, year, or month, year. If more than one date appears on the report, use date of publication.

7a. TOTAL NUMBER OF PAGES: The total page count should follow normal pagination procedures, i.e., enter the number of pages containing information.

7b. NUMBER OF REFERENCES: Enter the total number of references cited in the report.

8a. CONTRACT OR GRANT NUMBER: If appropriate, enter the applicable number of the contract or grant under which the report was written.

8b, 8c, & 8d. PROJECT NUMBER: Enter the appropriate military department identification, such as project number, subproject number, system numbers, task number, etc.

9a. ORIGINATOR'S REPORT NUMBER(S): Enter the official report number by which the document will be identified and controlled by the originating activity. This number must be unique to this report.

9b. OTHER REPORT NUMBER(S): If the report has been assigned any other report numbers *(either by the originator or by the sponsor)*, also enter this number(s).

10. AVAILABILITY/LIMITATION NOTICES: Enter any limitations on further dissemination of the report, other than those imposed by security classification, using standard statements such as:

(1) "Qualified requesters may obtain copies of this report from DDC."

(2) "Foreign announcement and dissemination of this report by DDC is not authorized."

(3) "U. S. Government agencies may obtain copies of this report directly from DDC. Other qualified DDC users shall request through _____."

(4) "U. S. military agencies may obtain copies of this report directly from DDC. Other qualified users shall request through _____."

(5) "All distribution of this report is controlled. Qualified DDC users shall request through _____."

If the report has been furnished to the Office of Technical Services, Department of Commerce, for sale to the public, indicate this fact and enter the price, if known.

11. SUPPLEMENTARY NOTES: Use for additional explanatory notes.

12. SPONSORING MILITARY ACTIVITY: Enter the name of the departmental project office or laboratory sponsoring *(paying for)* the research and development. Include address.

13 ABSTRACT. Enter an abstract giving a brief and factual summary of the document indicative of the report, even though it may also appear elsewhere in the body of the technical report. If additional space is required, a continuation sheet shall be attached.

It is highly desirable that the abstract of classified reports be unclassified. Each paragraph of the abstract shall end with an indication of the military security classification of the information in the paragraph, represented as *(TS)*, *(S)*, *(C)* or *(U)*.

There is no limitation on the length of the abstract. However, the suggested length is from 150 to 225 words.

14 KEY WORDS: Key words are technically meaningful terms or short phrases that characterize a report and may be used as index entries for cataloging the report. Key words must be selected so that no security classification is required. Identifiers, such as equipment model designation, trade name, military project code name, geographic location, may be used as key words but will be followed by an indication of technical context. The assignment of links, rules, and weights is optional.